The Aeronautical Journal (2024), 1–47
doi:10.1017/aer.2024.50

ROYAL AERONAUTICAL SOCIETY

RESEARCH ARTICLE

Non-overshooting sliding mode for UAV control

X. Wang[1] and X. Mao[2]

[1]Aerospace Engineering, University of Nottingham, Nottingham, United Kingdom
[2]Advanced Research Institute of Multidisciplinary Sciences, Beijing Institute of Technology, Beijing, China
Corresponding author: X. Wang; Email: wangxinhua04@gmail.com

Received: 5 August 2023; **Revised:** 17 March 2024; **Accepted:** 22 April 2024

Keywords: non-overshooting sliding mode; global non-overshooting stability; non-overshooting reachability; smoothed non-overshooting controller; UAV trajectory tracking

Abstract

For a class of uncertain systems, a non-overshooting sliding mode control is presented to make them globally exponentially stable and without overshoot. Even when the unknown stochastic disturbance exists, and the time-variant reference trajectory is required, the strict non-overshooting stabilisation is still achieved. The control law design is based on a desired second-order sliding mode (2-sliding mode), which successively includes two bounded-gain subsystems. Non-overshooting stability requires that the system gains depend on the initial values of system variables. In order to obtain the global non-overshooting stability, the first subsystem with non-overshooting reachability compresses the initial values of the second subsystem to a given bounded range. By partitioning these initial values, the bounded system gains are determined to satisfy the robust non-overshooting stability. In order to reject the chattering in the controller output, a tanh-function-based sliding mode is developed for the design of smoothed non-overshooting controller. The proposed method is applied to a UAV trajectory tracking when the disturbances and uncertainties exist. The control laws are designed to implement the non-overshooting stabilisation in position and attitude. Finally, the effectiveness of the proposed method is demonstrated by the flying tests.

Nomenclature

$e(t)$	system variable of error form
$e^{(n)}(t)$	the n -th derivative of $e(t)$
$f(\cdot)$	system function
$g(\cdot)$	system function
k_p	proportional gain of PID controller
k_i	integral gain of PID controller
k_d	derivative gain of PID controller
$e_1(t)$	sliding variable or error variable
$e_2(t)$	sliding variable or error variable
k_1	parameter of sliding mode or controller parameter
k_2	parameter of sliding mode or controller parameter
ρ	parameter of sliding mode or controller parameter
$d(t)$	disturbance or system uncertainty
L_d	upper bound of $d(t)$
$\sigma(t)$	sliding function
$x_1(t)$	system state
$x_2(t)$	system state
$u(t)$	controller
$\delta(t)$	system uncertainty or disturbance
$x_d(t)$	reference
$\dot{x}_d(t)$	derivative of reference

m	mass of UAV
g	gravity of acceleration
l	rotor distance to gravity centre
J_ϕ	moment of inertia about roll
x	position in x direction
y	position in y direction
z	position in z direction
ϕ	roll angle
θ	pitch angle
ψ	yaw angle
J_θ	moment of inertia about pitch
J_ψ	moment of inertia about yaw
b	rotor force coefficient
k	rotor torque coefficient
F_i	thrust force by rotor i
Q_i	reactive torque of rotor i
k_x	drag coefficients of UAV in x direction
k_y	drag coefficients of UAV in y direction
k_z	drag coefficients of UAV in z direction
k_ϕ	drag coefficients of UAV about roll
k_θ	drag coefficients of UAV about pitch
k_ψ	drag coefficients of UAV about yaw
Δ_x	uncertainty in x direction
Δ_y	uncertainty in y direction
Δ_z	uncertainty in z direction
Δ_ϕ	uncertainty about roll
Δ_θ	uncertainty about pitch
Δ_ψ	uncertainty about yaw

1.0 Introduction

This paper considers robust non-overshooting stabilisation for a class of dynamical systems with stochastic disturbance and application to UAV flight control. Control without overshoot is very important for many industrial control systems [1–3], for example, aircraft safe landing, automated vehicle safety control and manufacturing process control, etc. In a control system, overshoot makes the actual behaviour exceed its target, and it may bring the devastating results. Therefore, in order to guarantee the safety control, a known reference needs to be tracked without overshoot, i.e. non-overshooting stabilisation is required. For control systems, in addition to reduce the overshoot and oscillations in the system outputs, the effect from the disturbance or uncertainty also needs to be avoided. Furthermore, a smoothed control law is helpful to improve the system response and reduce the actuator chattering.

Proportional–integral–derivative (PID) control is very popular for many industrial control systems because of its simplicity and its acceptable control performance [4, 5]. However, PID control has some disadvantages; for example, sensitive to the disturbance and uncertainty types, adverse effect by the time-variant references, overshoot existence because of integral windup or integration saturation. Theoretically, PID control can completely reject the effect from an unknown constant disturbance because of the integration term. If the disturbance is slowly time-varying, through increasing the control gains, the disturbance effect can be reduced to some extent. For a fast time-varying disturbance or nonlinear system uncertainty, PID control performance is affected obviously. In addition, PID control is usually used to control a system with step reference for good performance. If the time-variant reference is required, the feedforward term including reference derivatives information should be added in the PID controller. For PID or proportional–integral (PI) control, the large initial error may bring the phenomenon of integral windup, and a relatively long-time overshoot exits in the system output. There are some methods to reduce overshoot in system output: the pole-placement or pole-zero configuration

https://doi.org/10.1017/aer.2024.50 Published online by Cambridge University Press

methods [6, 7], the optimisation approach to minimise overshoot [8], the compensation-based method [9, 10], the characteristic ratio assignment method [11], the iterative technique based on gradient descent-like procedure [12], the eigenvector placement technique to construct an invariant set [13]. They are mainly used for the step reference non-overshooting tracking in the linear systems. However, they still cannot overcome the effect from the time-varying disturbances or nonlinear system uncertainties, and these time-varying disturbances may bring overshoot or oscillations in the system outputs.

Sliding mode is also widely used in many industrial applications due to its strong robustness against the bounded stochastic disturbances or uncertainties, especially for aircraft navigation and control: the robust controller [14], the robust observer [15] and the signal corrector [16]. However, chattering in sliding mode affects its output performance, and overshoot is inevitable for the usual sliding mode control systems. Some methods were proposed to reduce overshoot and chattering, and keep the robustness property of sliding mode control [17–20]. In [17], for the systems with the parameter uncertainties and the matched disturbances, an adaptive sliding mode was designed to create the non-overshooting responses over the selected output variables. In Ref. [18], a cascade sliding mode-PID control was presented to get the non-overshooting time responses for a step reference. In Refs [19, 20], for a linear time-invariant systems with the matched disturbance, the integral sliding mode technique along with the Moore's eigenstructure assignment was used to make the system stable with non-overshooting behaviour. For the above methods, not only the upper bound of disturbance should be known, but also the upper bound information of disturbance derivatives is required. For some cases, the non-overshooting controllers with the observers were presented for the systems with the disturbances [21, 22]. The observers were designed to estimate the disturbances, and the estimations were used for the non-overshooting stabilisation. However, only the step reference was considered, and the disturbance was assumed to be constant. Furthermore, the overshoot may exist in the estimation from the observer, and the non-overshooting control performance is affected adversely.

Recent years, non-overshooting stabilisation for the nonlinear systems with disturbance was developed [23–26]. In Ref. [23], a non-overshooting control was presented for a class of nonlinear system under the condition that the initial value of the system output was strictly required below the initial value of the reference trajectory. The approximately non-overshooting performance was achieved by appropriately choosing the control gains under the deterministic disturbances. In Ref. [24], a controller was designed for a class of nonlinear systems to make the mean of the system output asymptotically track a given trajectory without overshoot, i.e. the mean-nonovershooting tracking was achieved. Furthermore, the initial value of the system output has the same constraint as that in Ref. [23]. In Refs [25, 26], the non-overshooting stabilisers were designed for a class of nonlinear systems that were input-output linearisable with a full relative degree, and the matched disturbances were considered. The bounded measurable disturbances should satisfy the two inequalities including the initial values of variables, and it was required to be continuous in the system variables [26]. In addition, the above non-overshooting control methods are locally stable.

In this paper, for a class of uncertain systems, a method of globally exponentially stable control without overshoot is proposed. The design of control law is based on a global non-overshooting 2-sliding mode of error form. Non-overshooting stability requires that the system gains depend on the initial values of system variables, making the system locally stable. In order to achieve the global non-overshooting stability and avoid the excessively large system gains, the 2-sliding mode consists of two bounded-gain subsystems. The implementation of global non-overshooting stability is through the successive connection of the first subsystem with non-overshooting reachability and the second subsystem with locally non-overshooting stability. The first subsystem enables the sliding variables to reach a given bounded range without overshoot within a finite time. The boundary of this range serves as the initial values for the second subsystem. Through partitioning these initial values, the sliding variables are analytically expressed, and in each zone, the bounded system parameters are determined to achieve the non-overshooting stability. For the second subsystem, the sliding variables are attracted without overshoot onto a non-overshooting sliding surface (i.e. the sliding variables are made to satisfy a linear non-overshooting convergence law). Thus, the sliding variables converge exponentially to zero, and

https://doi.org/10.1017/aer.2024.50 Published online by Cambridge University Press

there is no overshoot for the first sliding variable. The influence of the bounded stochastic disturbance or uncertainty is rejected completely due to the sliding mode gain coverage. The disturbance or uncertainty is only required to be bounded. Also, the 2-sliding mode can separate the measurement noise from the sliding variables, and it makes the variables smoothed. To implement the trajectory non-overshooting tracking, it is only required that the second-order derivative of reference trajectory is bounded. In order to reject the chattering in the controller output, a tanh-function-based sliding mode is developed to get the smoothed non-overshooting controller.

The rationality of the proposed non-overshooting sliding mode controller in this paper incudes: (1) the structure of the two successive subsystems, which have the non-overshooting reachability and the non-overshooting stability respectively, can achieve global non-overshooting stability; (2) the initial value partitioning of the second subsystem is to determine the analytical expressions for the sliding variables, so that the conditions on non-overshooting stability can be obtained; (3) the sliding mode gains can be assigned to completely eliminate the influence of bounded stochastic disturbance. The advantages of the proposed method are: (1) the robust and global non-overshooting stability even in the presence of bounded stochastic disturbance; (2) no restriction on the system initial values; (3) the bounded and smoothed controller to be easily performed by the actuators.

For flight control, for example, spacecraft, hypersonic vehicle or UAV control, sliding mode control plays an important role [27–29]. However, overshoot or oscillations exist for the traditional sliding mode control methods. In the high-speed or high-manoeuverability flight conditions, overshoot or oscillations in attitude control may affect the flight performance and cause the safety issues. In fact, at a supersonic flying speed, the angles of attack of the aerodynamic surfaces are usually very small. The overshoot of the system output will cause these angles of attack large and irregular, resulting in the unstable flight. Therefore, the non-overshooting control is necessary for these aircrafts to implement the safe and maneuvering flight. The robust non-overshooting control proposed in this paper can overcome the overshoot issue, and the strict non-overshooting stability can be achieved even in the presence of bounded stochastic disturbance or system uncertainty. Importantly, the bounded-gain and smoothed sliding controller is fit for many actuators.

The proposed method is applied to a UAV non-overshooting control. In the UAV flight test, some adverse situations are considered: only a simple model is constructed; the system uncertainties and the bounded unknown stochastic disturbances exist; noise is in the measurements of position and attitude; and the reference includes the multi-segment trajectory. The control laws based on the non-overshooting sliding mode are designed to drive the UAV to achieve the flight mission. The control system can implement the agile and non-overshooting tracking for the complex reference trajectory. Furthermore, even when the reference suddenly changes or jumps, i.e. the reference trajectory is discontinuous, the controller parameters can be updated to keep the non-overshooting stabilisation through the parameter regulation conditions.

Compared with the research results in the existing relevant literature, the contributions of this paper include: (1) even with the presence of stochastic disturbances and the requirement of time-variant reference trajectories, the strict non-overshooting stability can still be achieved; (2) the stability is global, and the system gains are bounded; (3) the stochastic disturbances are only required to be bounded; (4) there is no restriction on the initial values of the systems; (5) due to the filter-corrector property of the sliding mode surface, the noise can be fully separated from the sliding variables, even when the frequency bands of the variables and noise overlap; (6) the controller output is bounded and is smoothed, and it is easily performed by the actuators.

2.0 Problem description and analysis

The problem considered in this paper is for system safety control to implement non-overshooting stabilisation, even the unknown stochastic disturbance exists, and the time-variant reference is required. Overshoot means that signal passes over or exceeds its target, and it affects the safety control adversely.

https://doi.org/10.1017/aer.2024.50 Published online by Cambridge University Press

We know that, the control performance of a system is determined by its closed-loop error system after a controller is selected. Equivalently speaking, controller design is to determine a control law to turn the open-loop error system into a desired stable system of error form. The control performance is determined by the desired stable system. The controller is a connection between the open-loop error system and the desired stable system.

Therefore, when it is difficult to design a controller to make a system stable and without overshoot, we can construct a desired stable system with non-overshooting and robust properties. Then, from the relation between the open-loop error system and the desired stable system, the controller is solved.

A conclusion on controller design based on desired stable system is introduced as follows.

2.1 Controller design and desired stable system

Conclusion 2.1 (*Controller design based on desired stable system*):

A dynamical system of error form is considered as follows:

$$e^{(n)}(t) = g\left(e(t), \dot{e}(t), \cdots, e^{(n-1)}(t), t\right) + u(t) + d(t) \tag{1}$$

where, $e(t)$ is the system error variable, and $\dot{e}(t), \cdots, e^{(n)}(t)$ are the derivatives of $e(t)$; $g(\cdot)$ is the known function; $u(t)$ is the control input; and $d(t)$ is the unknown disturbance or uncertainty of any kind. If the system

$$e^{(n)}(t) = f\left(e(t), \dot{e}(t), \cdots, e^{(n-1)}(t), t\right) + d(t) \tag{2}$$

is already stable even disturbance $d(t)$ exists, i.e.

$$\lim_{t\to\infty} e^{(i)}(t) = 0, i = 0, 1, \cdots, n-1 \tag{3}$$

where, $f(\cdot)$ is the known function, then, in order to make system (1) stable, the controller can be selected as

$$u(t) = f\left(e(t), \dot{e}(t), \cdots, e^{(n-1)}(t), t\right) - g\left(e(t), \dot{e}(t), \cdots, e^{(n-1)}(t), t\right) \tag{4}$$

In fact, system (2) is already stable without control. If we can select controller $u(t)$ to turn system (1) into system (2), then, the system (1) will become stable. Because the left sides of (1) and (2) are same, we just make the right sides of (1) and (2) equal, i.e.

$$g\left(e(t), \dot{e}(t), \cdots, e^{(n-1)}(t), t\right) + u(t) + d(t) = f\left(e(t), \dot{e}(t), \cdots, e^{(n-1)}(t), t\right) + d(t) \tag{5}$$

Then, through solving the equality (5), the disturbance $d(t)$ is canceled out, and we get the controller (4).

Remark 2.1: For system (1) with controller (4), system (2) determines its stability, transient process and robustness. Therefore, for a dynamical control system, we can use a desired stable system to determine the controller and analyse the performance of control system. Importantly, for safety control, if the desired stable system has the non-overshooting property, then the dynamical control system has the same performance.

2.2 PID/PI desired stable system

PID/PI control is popular for many industrial control systems. Ideally, PID or PI control can completely reject the effect of constant disturbance when stabilising a system. The desired stable system in PID form is a third-order system, and the overshoot often happens. Especially, a large overshoot exists due to the windup effect or the integration saturation. We have the following two Lemmas.

Lemma 2.1 (PID desired stable system with unknown constant disturbance)*: For system*

$$\ddot{e}(t) = -k_p e(t) - k_i \int_0^t e(\tau)d\tau - k_d \dot{e}(t) + d \tag{6}$$

https://doi.org/10.1017/aer.2024.50 Published online by Cambridge University Press

where, d is any unknown constant disturbance, if k_p, k_i and k_d are selected to make the real parts of all the roots of the characteristic equation $s^3 + k_d s^2 + k_p s + k_i = 0$ negative, then, system (6) is exponentially stable, and

$$\lim_{t\to\infty} e(t) = 0, \lim_{t\to\infty} \dot{e}(t) = 0, \text{ and } \lim_{t\to\infty} k_i \int_0^t e(\tau)d\tau = d \tag{7}$$

The proof of Lemma 2.1 is presented in Appendix. ■

Remark 2.2 (*PID control for second-order systems*): Ideally, PID controller is used for the control of a second-order system with unknown constant disturbance (but not time-varying disturbance). For the second-order system of error form

$$\ddot{e}(t) = -g(t) - u(t) + d \tag{8}$$

the system (6) is selected as the desired stable system. We select the right sides of (6) and (8) equal, i.e.

$$-g(t) - u(t) + d = -k_p e(t) - k_i \int_0^t e(\tau)d\tau - k_d \dot{e}(t) + d \tag{9}$$

Then, solving the equality (9), the disturbance d is canceled out, and we get the controller:

$$u(t) = k_p e(t) + k_i \int_0^t e(\tau)d\tau + k_d \dot{e}(t) - g(t) \tag{10}$$

From (66), the closed-loop error system is a third-order system, the combination of three roots of $s^3 + k_d s^2 + k_p s + k_i = 0$ determines the stability and transient process, and the overshooting response often happens.

For PID control, if the large initial error of system output variable exist, then a relatively large long-time overshoot may happen due to the integral windup. PID control can only completely reject the effect of constant disturbance and make $\lim_{t\to\infty} e(t) = 0$ and $\lim_{t\to\infty} \dot{e}(t) = 0$. In addition, for a time-varying disturbance, PID control can only make the system approximately stable. Even the parameter regulation methods are used to implement the non-overshooting stabilisation, the disturbance is still assumed to be constant. If disturbance is fast time-varying, then the control performance becomes worse, and the overshoot and oscillations deteriorate.

Lemma 2.2 (PI desired stable system with unknown constant disturbance): *For system*

$$\dot{e}(t) = -k_p e(t) - k_i \int_0^t e(\tau)d\tau + d \tag{11}$$

where, d is any unknown constant disturbance, if k_p and k_i are selected to make the real parts of all the roots of the characteristic equation $s^2 + k_p s + k_i = 0$ negative, then system is exponentially stable, and

$$\lim_{t\to\infty} e(t) = 0, \text{ and } \lim_{t\to\infty} k_i \int_0^t e(\tau)d\tau = d \tag{12}$$

The proof of Lemma 2.2 is presented in Appendix. ■

Remark 2.3: Ideally, PI controller is used for the control of a first-order system with unknown constant disturbance. For the first-order system of error form

$$\dot{e}(t) = -g(t) - u(t) + d \tag{13}$$

the system (11) is selected as the desired stable system. We select the right sides of (11) and (13) equal, i.e.

$$-g(t) - u(t) + d = -k_p e(t) - k_i \int_0^t e(\tau)d\tau + d \tag{14}$$

Then, solving the equality (14), the disturbance d is canceled out, and we get the controller:

$$u(t) = k_p e(t) + k_i \int_0^t e(\tau)d\tau - g(t) \tag{15}$$

https://doi.org/10.1017/aer.2024.50 Published online by Cambridge University Press

From (72), the closed-loop error system is a second-order system, the combination of two roots of $s^2 + k_p s + k_i = 0$ determines the stability and transient process, and sometimes overshooting response happens. Furthermore, due to the integral windup, the overshoot happens. Strictly, PI control can only reject the effect of constant disturbance and make $\lim_{t\to\infty} e(t) = 0$. For a time-varying disturbance, PI control can only make the system approximately stable.

2.3 Performance metrics to evaluate the control methods

In the view of the problems under consideration, here, we give the performance metrics for evaluating the proposed control methods: (1) global non-overshooting stability; (2) robustness against the bounded stochastic disturbances; (3) precision and maneuverability for reference trajectory tracking; (4) non restriction on the system initial values.

3.0 Robust non-overshooting 2-sliding mode

3.1 Configuration of robust non-overshooting 2-sliding mode with global stability

Before we present the design of non-overshooting control for a class of uncertain systems, we create a desired non-overshooting 2-sliding mode system. Non-overshooting stability requires that the system gain depends on the initial values of the system variables. When the initial value amplitudes are large, the system gain also becomes large. In order to achieve the global non-overshooting stability and the bounded system gain, the 2-sliding mode consists of two successive subsystems. The first subsystem with non-overshooting reachability enables the sliding variables to reach a given bounded range. This range boundary serves as the initial condition of the second subsystem and makes the determined system gain bounded. The second subsystem has the property of local non-overshooting stability, such that the sliding variables converge to zero, and no overshoot exists for the first sliding variable. The flow chart of 2-sliding mode is shown in Fig. 1(a).

The configuration of non-overshooting 2-sliding mode with two subsystems is expressed by

$$\begin{aligned} \dot{e}_1(t) &= e_2(t) \\ \dot{e}_2(t) &= \begin{cases} f_1\left[e_1(t)\,, e_2(t) + e_{2c}\mathrm{sign}(e_1(t))\right] + d(t), \mathrm{if}|e_1(t)| > e_{1c}; \\ f_2[e_1(t)\,, e_2(t)] + d(t), \mathrm{if}|e_1(t)| \le e_{1c} \end{cases} \end{aligned} \tag{16}$$

where, the gains of functions $f_1[\cdot]$ and $f_2[\cdot]$ are bounded; $d(t)$ is the bounded disturbance; $e_{1c} > 0$ and $e_{2c} > 0$ make the system gains bounded. The sliding variables $e_1(t)$ and $e_2(t)$ experience the following convergence process:

$$\begin{cases} e_1(t) \text{ reaches } e_{1c}\ \mathrm{sign}(e_1(t)) \text{ without overshoot and } e_2(t) \to -e_{2c}\ \mathrm{sign}(e_1(t))\,, \text{if } |e_1(t)| > e_{1c} \\ e_1(t) \to 0 \text{ without overshoot and } e_2(t) \to 0, \text{if } |e_1(t)| \le e_{1c} \end{cases} \tag{17}$$

The convergence process of sliding variables is shown in Fig. 1(b):

(1) The first subsystem (*with robust non-overshooting reachability*): its gain is bounded; it makes $e_1(t)$ reach the given range $|e_1(t)| \le e_{1c}$ without overshoot, and $e_2(t)$ approaches to the assigned $-e_{2c}\ \mathrm{sign}\,(e_1(t))$ which is opposite to $e_1(t)$; the bounded disturbance $d(t)$ can be rejected completely; and then the first subsystem switches to the second subsystem, which it has the initial values $e_1(t_c)$ and $e_2(t_c)$.

(2) The second subsystem (*with robust non-overshooting stability*): its bounded gain is determined from the initial values $e_1(t_c)$ and $e_2(t_c)$; the sliding variables $e_1(t)$ and $e_2(t)$ converge to zero, and no overshoot exists for $e_1(t)$; moreover, the bounded disturbance $d(t)$ can be rejected completely.

Two Theorems on the explicit forms of robust non-overshooting 2-sliding mode are presented as follows.

https://doi.org/10.1017/aer.2024.50 Published online by Cambridge University Press

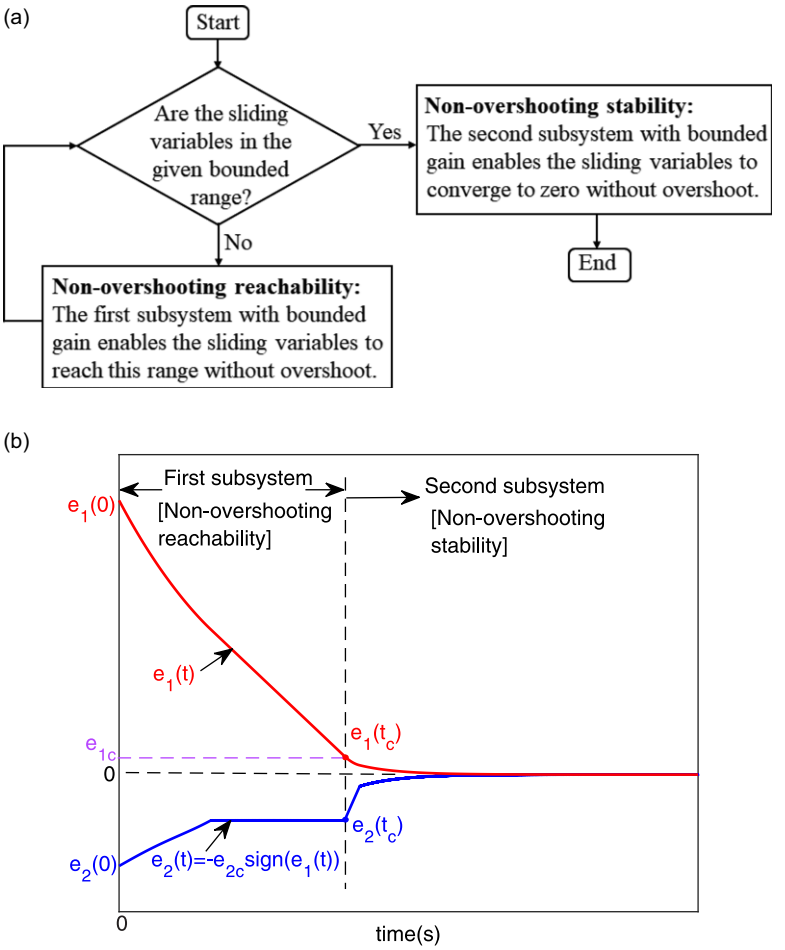

Figure 1. *Configuration of globally non-overshooting 2-sliding mode. (a) Flow chart of 2-sliding mode. (b) Convergence process of sliding variables.*

3.2 Design of non-overshooting sliding mode system

Theorem 3.1 (Robust non-overshooting 2-sliding mode): *The 2-sliding mode system is as follows:*

$$\begin{aligned}\dot{e}_1(t) &= e_2(t)\\ \dot{e}_2(t) &= \begin{cases} -k_c \mathrm{sign}\left[e_2(t) + e_{2c}\mathrm{sign}(e_1(t))\right] + d(t), \text{if} |e_1(t)| > e_{1c};\\ -k_2 \mathrm{sign}[e_2(t) + k_1 e_1(t)] + d(t), \text{if} |e_1(t)| \le e_{1c} \end{cases}\end{aligned} \tag{18}$$

where, $e_1(t)$ and $e_2(t)$ are the sliding variables; the bounded unknown disturbance $d(t)$ satisfies $\sup_{t\in[0,\infty)} |d(t)| \le L_d < \infty$; $k_c > L_d$; $e_{1c} \in (0, k_{2M} - L_d)$, $e_{2c} \in \left(e_{1c}, \sqrt{(k_{2M} - L_d)\, e_{1c}}\right]$, and $k_{2M} > L_d$ is the up-bound of k_2 from the system gain limitation; $e_1(t_c)$ and $e_2(t_c)$ are the initial values of $e_1(t)$ and $e_2(t)$ respectively when $|e_1(t)| \le e_{1c}$; and

$$k_1 \in \begin{cases} \left(0, \frac{|e_2(t_c)|}{|e_1(t_c)|}\right), \text{if } e_1(t_c)\, e_2(t_c) < 0 \text{ and } |e_1(t_c)| < |e_2(t_c)|;\\ \left(\frac{|e_2(t_c)|}{|e_1(t_c)|}, \infty\right), \text{if } e_1(t_c)\, e_2(t_c) < 0 \text{ and } |e_1(t_c)| \ge |e_2(t_c)|;\\ (0, \infty), \text{if others} \end{cases} \tag{19}$$

https://doi.org/10.1017/aer.2024.50 Published online by Cambridge University Press

$$k_2 > \begin{cases} \max\left\{k_1\,|e_2(t_c)| + L_d,\ \frac{e_2^2(t_c)}{2|e_1(t_c)|} + L_d\right\}, \text{if } e_1(t_c)\,e_2(t_c) < 0 \text{ and } |e_1(t_c)| < |e_2(t_c)|\,; \\ \max\left\{k_1\,|e_2(t_c)| + L_d,\ \frac{k_1^2}{3}\left(|e_1(t_c)| + \sqrt{e_1^2(t_c) + 3\left(\frac{e_2(t_c)}{k_1}\right)^2}\right) + L_d\right\}, \text{if others} \end{cases} \tag{20}$$

Then, we get the linear convergence law $\dot{e}_1(t) = -k_1 e_1(t)$ *(i.e., sliding surface* $e_2(t) + k_1 e_1(t) = 0$*), i.e. the system (18) is globally exponentially stable, and*

$$\lim_{t\to\infty} e_1(t) = 0 \text{ and } \lim_{t\to\infty} e_2(t) = 0 \tag{21}$$

In addition, the convergence of variable $e_1(t)$ *is non-overshooting.*
The proof of Theorem 3.1 is presented in Appendix. ■

Remark 3.1 (Performance analysis of sliding mode (18) with conditions (19) and (20)):

(1) Globally exponential stability and no overshoot. During the whole transient process, both $e_1(t)$ and $e_2(t)$ converge to zero, and no overshoot exists in $e_1(t)$:

(i) Firstly, there exists a finite time $t_c > 0$, for $t \geq t_c$, the first subsystem enables $e_1(t)$ to reach $|e_1(t)| \leq e_{1c}$ without overshoot; meanwhile, $e_2(t)$ gets to $e_{2c}\text{sign}(e_1(t))$; then, the first subsystem switches to the second subsystem.

(ii) Secondly, for the second subsystem within the range $|e_1(t)| \leq e_{1c}$, from its initial values $e_1(t_c)$ and $e_2(t_c)$, there exists a finite time $t_s > 0$, for $t \geq t_c + t_s$, the variables $_1(t)$ and $e_2(t)$ are attracted without overshoot onto the sliding surface $\sigma(t) = e_2(t) + k_1 e_1(t) = 0$, and the sliding function $\sigma(t)$ and the sliding variable $e_1(t)$ are non-overshooting during $t \in [t_c, t_c + t_s)$; because $\dot{e}_1(t) = e_2(t)$, the linear convergence law $\dot{e}_1(t) = -k_1 e_1(t)$ is achieved; therefore, for $t \geq t_c + t_s$, $e_1(t)$ and $e_2(t)$ are exponentially convergent, and no overshoot exists in $e_1(t)$. Therefore, it is a non-overshooting convergence process.

(2) Complete rejection of bounded stochastic disturbance/uncertainty. Disturbances or uncertainties exist in many dynamic systems. For example, in a UAV flight, the aerodynamic disturbance exists from the crosswind, and the influences of unmodelled dynamic uncertainties are not avoidable in modeling. They perform to be stochastic and bounded. Therefore, we can define the disturbance or uncertainty $d(t)$ to satisfy $\sup_{t\in[0,\infty)} |d(t)| \leq L_d < \infty$. For the sliding mode (18), even the bounded disturbance $d(t)$ exists, the strict non-overshooting and exponential stability is still achieved, and $\lim_{t\to\infty} e_1(t) = 0$ and $\lim_{t\to\infty} e_2(t) = 0$. In fact, from (84) to (86) in the proof of Theorem 3.1, due to $k_c > L_d$ and $k_2 > L_d$ in the sliding mode, the influence of bounded disturbances or uncertainties can be completely rejected. Furthermore, for this sliding mode, the condition on the stochastic disturbance $d(t)$ is relax, and $d(t)$ is only required to be bounded.

(3) Bounded gain of the sliding mode. From (20), the selection of $e_{1c} \in (0, k_{2M} - L_d)$ (i.e., $e_{1c} = |e_1(t_c)|$) and $e_{2c} \in \left(e_{1c}, \sqrt{(k_{2M} - L_d)\,e_{1c}}\right]$ (i.e., $e_{2c} = |e_2(t_c)|$) makes $|e_1(t_c)|$, $|e_2(t_c)|$ and $\frac{e_2^2(t_c)}{2|e_1(t_c)|}$ all bounded. Therefore, k_2 is bounded, and the non-overshooting performance is guaranteed.

(4) Chattering phenomenon in the sliding variable $e_2(t)$. For the sliding mode (18), due to the switching functions in the $e_2(t)$ dynamic equation, chattering may exist in $e_2(t)$.

Remark 3.2 (*Parameter conditions that cause slow convergence*): For the selection of k_1 and k_2, we can use the partitioning $e_1(t_c)\,e_2(t_c) < 0$ and $e_1(t_c)\,e_2(t_c) \geq 0$, and we get

$$k_1 \in \begin{cases} \left(0, \frac{|e_2(t_c)|}{|e_1(t_c)|}\right), \text{if } e_1(t_c)\,e_2(t_c) < 0; \\ (0, \infty), \text{if others} \end{cases} \tag{22}$$

https://doi.org/10.1017/aer.2024.50 Published online by Cambridge University Press

$$k_2 > \begin{cases} \max\left\{k_1\,|e_2(t_c)| + L_d,\ \frac{e_2^2(t_c)}{2|e_1(t_c)|} + L_d\right\}, \text{if } e_1(t_c)\,e_2(t_c) < 0; \\ \max\left\{k_1\,|e_2(t_c)| + L_d,\ \frac{k_1^2}{3}\left(|e_1(t_c)| + \sqrt{e_1^2(t_c) + 3\left(\frac{e_2(t_c)}{k_1}\right)^2}\right) + L_d\right\}, \text{if others} \end{cases} \tag{23}$$

Thus, the system (18) is also globally exponentially stable, and no overshoot exists in $e_1(t)$.

However, for the second subsystem, when the initial values $e_1(t_c)$ and $e_2(t_c)$ of sliding variables are in the zones II-1 and IV-1, i.e., in $\{(e_1(t_c), e_2(t_c))\ |e_1(t_c)\,e_2(t_c) < 0$ and $|e_1(t_c)| \geq |e_2(t_c)|\}$, the slow convergence exists for sliding mode (18) with conditions (22) and (23), but it does not happen for sliding mode (18) with conditions (19) and (20). In fact:

(1) Slow convergence for sliding mode (18) with conditions (22) and (23): For the second subsystem, when the initial values of sliding variables are in the zones II-1 and IV-1, from (22), we know that $k_1 \in \left(0, \frac{|e_2(t_c)|}{|e_1(t_c)|}\right)$. $k_1 \in (0, 1)$ should be satisfied when $|e_1(t_c)| \geq |e_2(t_c)|$. Therefore, the $e_1(t)$ convergence may be slow due to the convergence law $\dot{e}_1(t) = -k_1 e_1(t)$.

(2) Fast convergence for sliding mode (18) with conditions (19) and (20): for the second subsystem, when the initial values of sliding variables are in the zones II-1 and IV-1, from (19), we know that $k_1 \in \left(\frac{|e_2(t_c)|}{|e_1(t_c)|}, \infty\right)$. Because $|e_1(t_c)| \geq |e_2(t_c)|$, we need to select $k_1 \geq 1$ for the convergence law $\dot{e}_1(t) = -k_1 e_1(t)$ to get a fast convergence.

3.3 Design of smoothed non-overshooting sliding mode system

In order to avoid $e_2(t)$ chattering in the sliding mode, the continuous functions are used in the sliding mode, and the following Theorem is presented.

Theorem 3.2 (Smoothed non-overshooting sliding mode): *The tanh-function-based 2-sliding mode system is as follows:*

$$\begin{aligned} \dot{e}_1(t) &= e_2(t) \\ \dot{e}_2(t) &= \begin{cases} -k_c \tanh\left[\rho_c(e_2(t) + e_{2c}\,\text{sign}(e_1(t)))\right] + d(t), \text{if} |e_1(t)| > e_{1c}; \\ -k_2 \tanh[\rho(e_2(t) + k_1 e_1(t))] + d(t), \text{if} |e_1(t)| \leq e_{1c} \end{cases} \end{aligned} \tag{24}$$

where, $e_1(t)$ and $e_2(t)$ are the sliding variables; the bounded unknown disturbance $d(t)$ satisfies $\sup_{t\in[0,\infty)} |d(t)| \leq L_d < \infty$; $e_{1c} \in (0, k_{2M} - L_d)$, $e_{2c} \in \left(e_{1c}, \sqrt{(k_{2M} - L_d)\,e_{1c}}\right]$, and $k_{2M} > L_d$ is the up-bound of k_2 from the system gain limitation; function

$$\tanh(\rho \cdot x) = \frac{e^{\rho \cdot x} - e^{-\rho \cdot x}}{e^{\rho \cdot x} + e^{-\rho \cdot x}} = 1 - \frac{2}{e^{2\rho \cdot x} + 1} \tag{25}$$

$$e_{1c} > 0, e_{2c} > 0, k_c > L_d, \rho_c \gg \frac{1}{2}\ln\frac{k_c + L_d}{k_c - L_d} \tag{26}$$

$e_1(t_c)$ and $e_2(t_c)$ are the initial values of $e_1(t)$ and $e_2(t)$ respectively when $|e_1(t)| \leq e_{1c}$; and

$$k_1 \in \begin{cases} \left(0, \frac{|e_2(t_c)|}{|e_1(t_c)|}\right), \text{if } e_1(t_c)\,e_2(t_c) < 0 \text{ and } |e_1(t_c)| < |e_2(t_c)|; \\ \left(\frac{|e_2(t_c)|}{|e_1(t_c)|}, \infty\right), \text{if } e_1(t_c)\,e_2(t_c) < 0 \text{ and } |e_1(t_c)| \geq |e_2(t_c)|; \\ (0, \infty), \text{if others} \end{cases} \tag{27}$$

https://doi.org/10.1017/aer.2024.50 Published online by Cambridge University Press

$$k_2 > \begin{cases} \max\left\{k_1 \left|e_2(t_c)\right| + L_d, \frac{e_2^2(t_c)}{2\left|e_1(t_c)\right|} + L_d\right\}, \text{if } e_1(t_c)\, e_2(t_c) < 0 \text{ and } \left|e_1(t_c)\right| < \left|e_2(t_c)\right|; \\ \max\left\{k_1 \left|e_2(t_c)\right| + L_d, \frac{k_1^2}{3}\left(\left|e_1(t_c)\right| + \sqrt{e_1^2(t_c) + 3\left(\frac{e_2(t_c)}{k_1}\right)^2}\right) + L_d\right\}, \text{if others} \end{cases} \tag{28}$$

$$\rho \gg \max\left\{\frac{1}{2k_1}, 1\right\} \ln\frac{k_2 + k_1 e_{2\max} + L_d}{k_2 - k_1 e_{2\max} - L_d} \tag{29}$$

and

$$e_{2\max} = \max\left\{\left|e_2(t_c)\right|, \frac{k_1}{3}\left[\left|e_1(t_c)\right| + \sqrt{e_1^2(t_c) + 3\left(\frac{e_2(t_c)}{k_1}\right)^2}\right]\right\} \tag{30}$$

Then:

(i) The effect of disturbances is rejected, and the variables $e_1(t)$ and $e_2(t)$ of system (24) are in the bounds as follows:

$$\lim_{t\to\infty}\left|e_1(t)\right| \le \frac{1}{2\rho k_1}\ln\frac{k_2 + k_1 e_{2\max} + L_d}{k_2 - k_1 e_{2\max} - L_d}, \text{and } \lim_{t\to\infty}\left|e_2(t)\right| \le \frac{1}{\rho}\ln\frac{k_2 + k_1 e_{2\max} + L_d}{k_2 - k_1 e_{2\max} - L_d} \tag{31}$$

In addition, the convergence of variable $e_1(t)$ is non-overshooting.

(ii) Specially, if ρ is large enough, i.e., $\rho \to +\infty$, then the system (24) becomes the ideal sliding mode (18), and we get

$$\lim_{t\to\infty}\lim_{\rho\to+\infty} e_1(t) = 0 \text{ and } \lim_{t\to\infty}\lim_{\rho\to+\infty} e_2(t) = 0 \tag{32}$$

The proof of Theorem 3.2 is presented in Appendix. ■

Remark 3.3 (*Smoothed and non-overshooting convergence for sliding mode* (24) *with* (25)∼(30)):

In addition to the non-overshooting convergence, the smoothed sliding mode system (24) has the following properties:

(1) Universal approximation: because $\lim_{\rho\to+\infty}\tanh(\rho\cdot x) = \text{sign}(x)$, the sliding mode system (24) is the smoothed approximation of ideal sliding mode system (18).

(2) Smoothed outputs of $e_1(t)$ and $e_2(t)$: Due to continuity in the sliding mode system (24), the outputs of both $e_1(t)$ and $e_2(t)$ are smoothed. For $-k_c\tanh\left[\rho_c(e_2(t) + e_{2c}\,\text{sign}(e_1(t)))\right] + d(t)$ in (24), the function $\text{sign}(e_1(t))$ does not change its sign due to continuity of $e_1(t)$ when $\left|e_1(t)\right| > e_{1c}$. Therefore, no chattering happens.

Remark 3.4 (*Parameters determination for the sliding mode system* (24))

For the algorithm calculation, we need to turn the inequality expressions of the parameters into the corresponding equalities, and the calculated maximum or minimum values of k_1 and k_2 are multiplied by the corresponding coefficients. The determination steps of e_{1c}, e_{2c}, k_c, ρ_c, k_1, k_2 and ρ are presented as follows.

Step 1: Get the initial errors $e_1(0)$ and $e_2(0)$.

Step 2: Select

$$\begin{aligned} e_{1c} &\in (0, k_{2M} - L_d), e_{2c} \in \left(e_{1c}, \sqrt{(k_{2M} - L_d)\, e_{1c}}\right] \\ k_c &\ge L_d, \rho_c = \rho_{c0}\frac{1}{2}\ln\frac{k_c + L_d}{k_c - L_d} \end{aligned} \tag{33}$$

where, $k_{2M} > L_d$ is the up-bound of k_2 limited from the system gain; and $\rho_{c0} > 1$

https://doi.org/10.1017/aer.2024.50 Published online by Cambridge University Press

Step 3: Determine the parameters k_1, k_2 and ρ through the following calculations.

$$k_1 = \begin{cases} \beta_{11} \frac{|e_2(t_c)|}{|e_1(t_c)|} \in \left(0, \frac{|e_2(t_c)|}{|e_1(t_c)|}\right), \text{if } e_1(t_c)\, e_2(t_c) < 0 \text{ and } |e_1(t_c)| < |e_2(t_c)|; \\ \beta_{12} \frac{|e_2(t_c)|}{|e_1(t_c)|} \in \left(\frac{|e_2(t_c)|}{|e_1(t_c)|}, \infty\right), \text{if } e_1(t_c)\, e_2(t_c) < 0 \text{ and } |e_1(t_c)| \geq |e_2(t_c)|; \\ \beta_{13} \in (0, \infty), \text{if others} \end{cases} \tag{34}$$

$$k_2 = \begin{cases} \beta_2 \max\left\{k_1 |e_2(t_c)| + L_d, \frac{e_2^2(t_c)}{2|e_1(t_c)|} + L_d\right\}, \text{if } e_1(t_c)\, e_2(t_c) < 0 \text{ and } |e_1(t_c)| < |e_2(t_c)|; \\ \beta_2 \max\left\{k_1 |e_2(t_c)| + L_d, \frac{k_1^2}{3}\left(|e_1(t_c)| + \sqrt{e_1^2(t_c) + 3\left(\frac{e_2(t_c)}{k_1}\right)^2}\right) + L_d\right\}, \text{if others} \end{cases} \tag{35}$$

where, $e_1(t_c)$ and $e_2(t_c)$ are the initial values of $e_1(t)$ and $e_2(t)$ respectively when $|e_1(t)| \leq e_{1c}$; $\beta_{11} \in (0, 1)$, $\beta_{12} > 1$ and $\beta_2 > 1$.

Adjustment of k_1:

$$k_1 = 1 \text{is selected if the calculated } k_1 \in (0, 1) \tag{36}$$

[*Note:* If k_1 is calculated to be $k_1 \in (0, 1)$, we can select $k_1 = 1$ for the convergence law $\dot{e}_1(t) = -k_1 e_1(t)$ to get a fast convergence. We find that $k_1 = 1$ always holds from the condition (27).]

For ρ, we select

$$\rho = \rho_0 \max\left\{\frac{1}{2k_1}, 1\right\} \ln\frac{k_2 + k_1 e_{2\max} + L_d}{k_2 - k_1 e_{2\max} - L_d} \tag{37}$$

where, $\rho_0 > 1$, and

$$e_{2\max} = \max\left\{|e_2(t_c)|, \frac{k_1}{3}\left[|e_1(t_c)| + \sqrt{e_1^2(t_c) + 3\left(\frac{e_2(t_c)}{k_1}\right)^2}\right]\right\} \tag{38}$$

4.0 Simulation examples on non-overshooting sliding mode

We use two examples to demonstrate the stability of the two non-overshooting sliding mode systems.

For sliding modes (18) and (24), we suppose:

the initial sliding variables $e_1(0) = 100$, $e_2(0) = -10$;

the disturbance $d(t) = 3 + 2\sin(0.3t)\sin(1.6t)$, and its upper bound $L_d = 5$.

Suppose the system gain $k_2 \leq k_{2M} = 20$.

Example 4.1: (Sliding mode (18) from Theorem 3.1):

From $e_{1c} \in (0, k_{2M} - L_d) = (0, 15)$, we select $e_{1c} = 2$. Then, we get $e_{2c} \in \left(e_{1c}, \sqrt{(k_{2M} - L_d)\, e_{1c}}\right] = \left(2, \sqrt{(20-5) \times 2}\right] = (2, 5.5]$. We select $e_{2c} = 5$. Select $k_c = 6 > L_d$.

Determination of sliding mode parameters k_1 *and* k_2 *according to the parameter determination steps* (34)∼(36):

$$k_1 = \begin{cases} 0.5 \frac{|e_2(t_c)|}{|e_1(t_c)|}, \text{if } e_1(t_c)\, e_2(t_c) < 0 \text{ and } |e_1(t_c)| < |e_2(t_c)|; \\ 2.3 \frac{|e_2(t_c)|}{|e_1(t_c)|}, \text{if } e_1(t_c)\, e_2(t_c) < 0 \text{ and } |e_1(t_c)| \geq |e_2(t_c)|; \\ 1 \in (0, \infty), \text{if others} \end{cases}$$

where, $e_1(t_c)$ and $e_2(t_c)$ are the initial values of $e_1(t)$ and $e_2(t)$ respectively when $|e_1(t)| \leq e_{1c}$.

https://doi.org/10.1017/aer.2024.50 Published online by Cambridge University Press

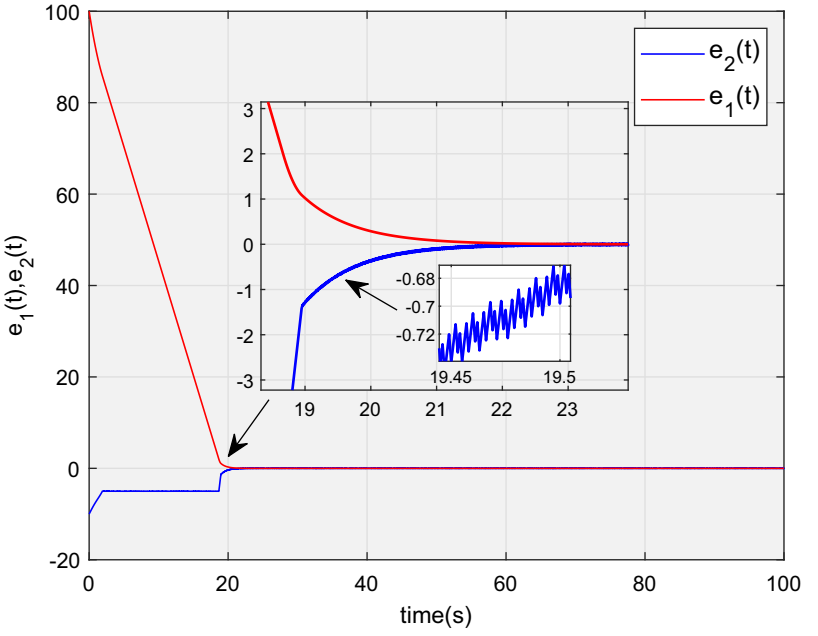

Figure 2. *Example 4.1 Sliding variables $e_1(t)$ and $e_2(t)$ of sliding mode (18).*

Adjustment of k_1: $k_1 = 1$ is selected if the calculated $k_1 \in (0, 1)$; and

$$k_2 = \begin{cases} 1.5 \max\left\{k_1 \left|e_2(t_c)\right| + L_d, \frac{e_2^2(t_c)}{2\left|e_1(t_c)\right|} + L_d\right\}, \text{if } e_1(t_c)\, e_2(t_c) < 0 \text{ and } \left|e_1(t_c)\right| < \left|e_2(t_c)\right|; \\ 1.5 \max\left\{k_1 \left|e_2(t_c)\right| + L_d, \frac{k_1^2}{3}\left(\left|e_1(t_c)\right| + \sqrt{e_1^2(t_c) + 3\left(\frac{e_2(t_c)}{k_1}\right)^2}\right) + L_d\right\}, \text{if others} \end{cases}$$

From the algorithm calculation for the above equations, we can obtain $k_1 = 1.25$ and $k_2 = 16.93$.

Figure 2 shows the plots of sliding variables $e_1(t)$ and $e_2(t)$. Even the time-varying disturbance exists, the non-overshooting convergence is implemented: the sign of $e_1(t)$ is always unchanged, and $\lim_{t\to\infty} e_1(t) = 0$ and $\lim_{t\to\infty} e_2(t) = 0$ hold. Also, we find that, small chattering exists in $e_2(t)$.

Example 4.2: (Smoothed sliding mode (24) from Theorem 3.2):

Similar to Example 4.1, select $e_{1c} = 2$, $e_{2c} = 5$, and $k_c = 6 > L_d$. Then, we get

$$\rho_c = 50\frac{1}{2}\ln\frac{k_c + L_d}{k_c - L_d} = 59.95$$

Determination of sliding mode parameters k_1, k_2 *and* ρ *according to the parameter determination steps* (34)∼(38):

Firstly, for determination of k_1 and k_2, we use the same algorithm steps as Example 3.1, and we can obtain $k_1 = 1.26$ and $k_2 = 16.95$. Secondly, for ρ, we have

$$e_{2\max} = \max\left\{\left|e_2(t_c)\right|, \frac{k_1}{3}\left[\left|e_1(t_c)\right| + \sqrt{e_1^2(t_c) + 3\left(\frac{e_2(t_c)}{k_1}\right)^2}\right]\right\}$$

$$\rho = 20 \max\left\{\frac{1}{2k_1}, 1\right\} \ln\frac{k_2 + k_1 e_{2\max} + L_d}{k_2 - k_1 e_{2\max} - L_d}$$

From the algorithm calculation for the above equations, we can read $\rho = 12.19$.

https://doi.org/10.1017/aer.2024.50 Published online by Cambridge University Press

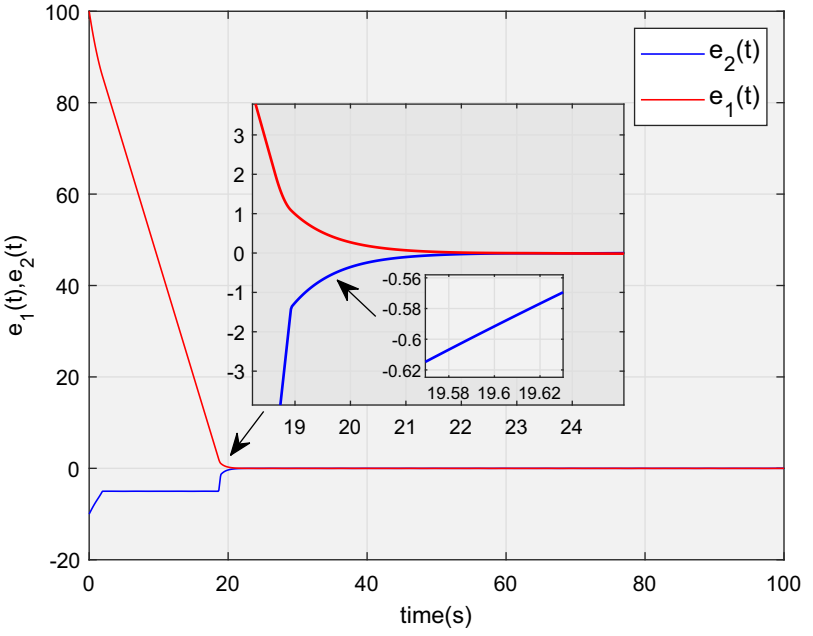

Figure 3. *Example 4.2 Sliding variables $e_1(t)$ and $e_2(t)$ of sliding mode (24).*

Figure 3 describes the plots of sliding variables $e_1(t)$ and $e_2(t)$. Even the time-varying disturbance exists, the sliding variables $e_1(t)$ and $e_2(t)$ converge to zero, and $e_1(t)$ convergence is non-overshooting. In addition, both $e_1(t)$ and $e_2(t)$ are smoothed.

5.0 Non-overshooting control for uncertain systems

5.1 Model of uncertain systems

The following uncertain system has a minimum number of states and inputs but retains the essential features that must be considered when designing control laws for many dynamical systems (e.g. UAV dynamics):

$$\begin{aligned} \dot{x}_1(t) &= x_2(t) \\ \dot{x}_2(t) &= h(t) + u(t) - \delta(t) \end{aligned} \tag{39}$$

where, $x_1(t)$ and $x_2(t)$ the system states; $h(t)$ is the known function; $u(t)$ is the control input; and $\delta(t)$ is the unknown time-varying disturbance or system uncertainty, and $\sup_{t\in[0,\infty)} |\delta(t)| \le L_\delta < \infty$. We consider to design a controller for the uncertain system (39) when the reference is time variant, and $x_1(t)$ tracking the reference is required to be non-overshooting.

5.2 Non-overshooting control for uncertain systems

Theorem 5.1 (Non-overshooting control based on sliding mode (18)): *For the uncertain system (39) with the time-variant reference $x_d(t)$, if the controller is selected as*

$$u(t) = \begin{cases} k_c \operatorname{sign}\big[e_2(t) + e_{2c} \operatorname{sign}(e_1(t))\big] - h(t), \text{if } |e_1(t)| > e_{1c} \\ k_2 \operatorname{sign}[e_2(t) + k_1 e_1(t)] - h(t), \text{if } |e_1(t)| \le e_{1c} \end{cases} \tag{40}$$

https://doi.org/10.1017/aer.2024.50 Published online by Cambridge University Press

then, the system is globally exponentially stable, $x_1(t)$ tracking $x_d(t)$ is non-overshooting, and

$$\lim_{t\to\infty} x_1(t) = x_d(t) \text{ and } \lim_{t\to\infty} x_2(t) = \dot{x}_d(t) \tag{41}$$

where, $e_1(t) = x_d(t) - x_1(t)$ and $e_2(t) = \dot{x}_d(t) - x_2(t)$; $\sup_{t\in[0,\infty)} |\ddot{x}_d(t)| \le L_x < \infty$, and $\sup_{t\in[0,\infty)} |\delta(t)| + \sup_{t\in[0,\infty)} |\ddot{x}_d(t)| \le L_d < \infty$; $k_c > L_d$; $e_{1c} \in (0, k_{2M} - L_d)$, $e_{2c} \in \left(e_{1c}, \sqrt{(k_{2M} - L_d)\, e_{1c}}\right]$, and $k_{2M} > L_d$ is the up-bound of k_2 from the system gain limitation; $e_1(t_c)$ and $e_2(t_c)$ are the initial values of $e_1(t)$ and $e_2(t)$ respectively when $|e_1(t)| \le e_{1c}$; and

$$k_1 \in \begin{cases} \left(0, \frac{|e_2(t_c)|}{|e_1(t_c)|}\right), \text{if } e_1(t_c)\, e_2(t_c) < 0 \text{ and } |e_1(t_c)| < |e_2(t_c)|; \\ \left(\frac{|e_2(t_c)|}{|e_1(t_c)|}, \infty\right), \text{if } e_1(t_c)\, e_2(t_c) < 0 \text{ and } |e_1(t_c)| \ge |e_2(t_c)|; \\ (0, \infty), \text{if others} \end{cases} \tag{42}$$

$$k_2 > \begin{cases} \max\left\{k_1 |e_2(t_c)| + L_d, \frac{e_2^2(t_c)}{2|e_1(t_c)|} + L_d\right\}, \text{if } e_1(t_c)\, e_2(t_c) < 0 \text{ and } |e_1(t_c)| < |e_2(t_c)|; \\ \max\left\{k_1 |e_2(t_c)| + L_d, \frac{k_1^2}{3}\left(|e_1(t_c)| + \sqrt{e_1^2(t_c) + 3\left(\frac{e_2(t_c)}{k_1}\right)^2}\right) + L_d\right\}, \text{if others} \end{cases} \tag{43}$$

The proof of Theorem 5.1 is presented in Appendix. ■

Remark 5.1 (*Non-overshooting control* (40)):

(1) *Non-overshooting of $x_1(t)$ tracking $x_d(t)$*: The sliding mode (18) is the desired stable system of error form, therefore, $e_1(t) = x_d(t) - x_1(t)$ converges to zero without overshoot. Thus, $x_1(t)$ tracking $x_d(t)$ is non-overshooting.

(2) *Complete rejection of the influence from bounded disturbance and time-variant reference:* For the uncertain system (39), the disturbance $\delta(t)$ and the second-order derivative of reference $x_d(t)$ are bounded, and $\sup_{t\in[0,\infty)} |\delta(t)| + \sup_{t\in[0,\infty)} |\ddot{x}_d(t)| \le L_d < \infty$ are satisfied. The parameters of controller (40) satisfy $k_c > L_d$ and (43). When selecting the controller (40), from (168) and (169) in the proof of Theorem 5.1, the closed-loop error system for (39) is the robust non-overshooting 2-sliding mode (18). Therefore, $\lim_{t\to\infty} x_1(t) = x_d(t)$ and $\lim_{t\to\infty} x_2(t) = \dot{x}_d(t)$, and there is no overshoot for $x_1(t)$ tracking $x_d(t)$.

(3) *Smoothed $x_1(t)$*: Due to the integral-chain structure of second-order sliding mode (18), $e_1(t)$ is smoothed. Therefore, for the control system, $x_1(t)$ is smoothed.

(4) *Chattering in the variable $x_2(t)$ and the controller $u(t)$*: For system (39), due to the controller of switching function exists in the $x_2(t)$ dynamic equation, chattering happens in $x_2(t)$. Also, the controller $u(t)$ in (40) is discontinuous, therefore, chattering exists in the controller output. The chattering in controller output will affect actuator performance adversely.

5.3 Smoothed non-overshooting control for uncertain systems

In order to reject chattering in the outputs of controller $u(t)$ and and variable $x_2(t)$, we present a smoothed control based on the sliding mode (24), and a Theorem is presented as follows.

Theorem 5.2 (Non-overshooting control based on smoothed sliding mode (24)): *For the uncertain system (39) with the time-variant reference $x_d(t)$, if the controller is selected as*

$$u(t) = \begin{cases} k_c \tanh\left[\rho_c(e_2(t) + e_{2c}\, \text{sign}(e_1(t)))\right] - h(t), \text{if } |e_1(t)| > e_{1c}; \\ k_2 \tanh[\rho(e_2(t) + k_1 e_1(t))] - h(t), \text{if } |e_1(t)| \le e_{1c} \end{cases} \tag{44}$$

https://doi.org/10.1017/aer.2024.50 Published online by Cambridge University Press

then, the system is globally exponentially stable, $x_1(t)$ tracking $x_d(t)$ is non-overshooting, and

$$\lim_{t\to\infty}|e_1(t)| \le \frac{1}{2\rho k_1}\ln\frac{k_2+k_1e_{2\max}+L_d}{k_2-k_1e_{2\max}-L_d}, \text{ and } \lim_{t\to\infty}|e_2(t)| \le \frac{1}{\rho}\ln\frac{k_2+k_1e_{2\max}+L_d}{k_2-k_1e_{2\max}-L_d} \tag{45}$$

where, $e_1(t)=x_d(t)-x_1(t)$ and $e_2(t)=\dot{x}_d(t)-x_2(t)$; $\sup_{t\in[0,\infty)}|\ddot{x}_d(t)|\le L_x<\infty$, and $\sup_{t\in[0,\infty)}|\delta(t)|+\sup_{t\in[0,\infty)}|\ddot{x}_d(t)|\le L_d<\infty$; $e_{1c}\in(0,k_{2M}-L_d)$, $e_{2c}\in\left(e_{1c},\sqrt{(k_{2M}-L_d)\,e_{1c}}\right]$, and $k_{2M}>L_d$ is the up-bound of k_2 from the system gain limitation;

$$k_c>L_d,\ \rho_c\gg\frac{1}{2}\ln\frac{k_c+L_d}{k_c-L_d} \tag{46}$$

$e_1(t_c)$ and $e_2(t_c)$ are the initial values of $e_1(t)$ and $e_2(t)$ respectively when $|e_1(t)|\le e_{1c}$; and

$$k_1\in\begin{cases}\left(0,\frac{|e_2(t_c)|}{|e_1(t_c)|}\right), \text{if } e_1(t_c)\,e_2(t_c)<0 \text{ and } |e_1(t_c)|<|e_2(t_c)|;\\ \left(\frac{|e_2(t_c)|}{|e_1(t_c)|},\infty\right), \text{if } e_1(t_c)\,e_2(t_c)<0 \text{ and } |e_1(t_c)|\ge|e_2(t_c)|;\\ (0,\infty), \text{if others}\end{cases} \tag{47}$$

$$k_2>\begin{cases}\max\left\{k_1\,|e_2(t_c)|+L_d,\frac{e_2^2(t_c)}{2|e_1(t_c)|}+L_d\right\}, \text{if } e_1(t_c)\,e_2(t_c)<0 \text{ and } |e_1(t_c)|<|e_2(t_c)|;\\ \max\left\{k_1\,|e_2(t_c)|+L_d,\frac{k_1^2}{3}\left(|e_1(t_c)|+\sqrt{e_1^2(t_c)+3\left(\frac{e_2(t_c)}{k_1}\right)^2}\right)+L_d\right\}, \text{if others}\end{cases} \tag{48}$$

$$\rho\gg\max\left\{\frac{1}{2k_1},1\right\}\ln\frac{k_2+k_1e_{2\max}+L_d}{k_2-k_1e_{2\max}-L_d} \tag{49}$$

with

$$e_{2\max}=\max\left\{|e_2(t_c)|,\frac{k_1}{3}\left[|e_1(t_c)|+\sqrt{e_1^2(t_c)+3\left(\frac{e_2(t_c)}{k_1}\right)^2}\right]\right\} \tag{50}$$

The proof of Theorem 5.2 is presented in Appendix. ■

Remark 5.2 (Smoothed non-overshooting control (44)):

(1) Non-overshooting of $x_1(t)$ tracking $x_d(t)$: The sliding mode (24) is the desired stable system of error form, therefore, no overshoot happens in $e_1(t)=x_d(t)-x_1(t)$. Thus, $x_1(t)$ tracking $x_d(t)$ is non-overshooting.

(2) Smoothed $x_1(t)$ and $x_2(t)$: Due to the use of continuous functions in sliding mode (24), both $e_1(t)$ and $e_2(t)$ are smoothed. Therefore, for the control system, $x_1(t)$ and $x_2(t)$ are smoothed.

(3) Smoothed controller $u(t)$: For system (39), the controller $u(t)$ in (44) is smoothed, and it is fit for the implementation by many actuators.

Remark 5.3 (*Rejection of measurement noise*):

For system (39) with the controller (40) or (44), the measurement noise is rejected on the sliding surface because of its filter-corrector property. Even when the frequency bands of the variables and noise overlap, the outputs of sliding surface are smoothed and are accurate.

In fact, suppose noise $n_1(t)$ and $n_2(t)$ exist in the measurements of $x_1(t)$ and $x_2(t)$, respectively. Then, for the sliding surface, we get

$$\dot{x}_d(t)-x_2(t)-n_2(t)+k_1[x_d(t)-x_1(t)-n_1(t)]=0 \tag{51}$$

i.e.

$$k_2(t)+k_1e_1(t)=k_1n_1(t)+n_2(t) \tag{52}$$

https://doi.org/10.1017/aer.2024.50 Published online by Cambridge University Press

Define the Laplace transforms $E_1(s) = L[e_1(t)]$, $E_2(s) = L[e_2(t)]$, $N_1(s) = L[n_1(t)]$, and $N_2(s) = L[n_2(t)]$. Taking Laplace transform for (52), we get

$$sE_1(s) + k_1E_1(s) = k_1N_1(s) + N_2(s) \tag{53}$$

i.e.

$$E_1(s) = \frac{k_1}{s+k_1}\left(N_1(s) + \frac{1}{k_1}N_2(s)\right) \tag{54}$$

where, $\frac{k_1}{s+k_1}$ is the form of first-order filter, and k_1 is the cut-off frequency of the filter. For the filter, the input is the noise, and the output is the system error. As long as k_1 is less than the minimum frequency of the noise, the noise will be rejected. From k_1 selection conditions, k_1 can be neither too large nor too small, for example, $k_1 = 1$ or $k_1 = 2$. Therefore, the noise $N_1(s) + \frac{1}{k_1}N_2(s)$ is rejected sufficiently, and the system error is reduced to be small enough.

Remark 5.4 (*Parameters regulation of the controller*):

(1) The parameter selection conditions (42) and (43) (i.e., (47) and (48)) make the system non-overshooting stable.

(2) $k_c > L_d$. If $|e_2(0)|$ is large, k_c should increase to reduce $|e_2(t)|$ effectively.

(3) k_1 determines the convergence rate of linear convergence law $\dot{e}_1(t) = -k_1e_1(t)$; from (54), k_1 also determines the filtering frequency band of the sliding mode. Therefore, k_1 should not be too small to keep a convergence rate of linear convergence law; and k_1 should not be too large to get a suitable frequency band for noise rejection.

(4) k_2 determines the convergence rate of the second subsystem; k_2 also keeps the signs of sliding function $\sigma(t) = e_2(t) + k_1e_1(t)$ and sliding variable $e_1(t)$ unchanged for $t \in [t_c, \infty)$; also, k_1 affects the selection of k_2.

(5) Because $|e_1(t_c)| = e_{1c}$ and $|e_2(t_c)| = e_{2c}$ when $t = t_c$, the selection of $e_{1c} \in (0, k_{2M} - L_d)$ and $e_{2c} \in \left(e_{1c}, \sqrt{(k_{2M} - L_d)\, e_{1c}}\right]$ makes $|e_1(t_c)|$, $|e_2(t_c)|$, $\frac{|e_2(t_c)|}{|e_1(t_c)|}$ and $\frac{e_2^2(t_c)}{2|e_1(t_c)|}$ are all bounded. Then, the bounded k_1 and k_2 are determined from (47) and (48).

(6) The selection of ρ from (49) affects the smoothness of system variables and controller output. Also, from (45), ρ affects the control precision. Therefore, the selection of ρ should balance the smoothness of variables and controller and the precision of control performance.

Remark 5.5 (*Steps on determination of non-overshooting controller)*

For the system (39), the flow chart of controller design is explained in Fig. 4. Furthermore, the the steps on controller determination are described as follows.

Step 1: Measure the system initial states, and get the initial errors $e_1(0)$ and $e_2(0)$.

Step 2: Select $e_{1c} \in (0, k_{2M} - L_d)$ and $e_{2c} \in \left(e_{1c}, \sqrt{(k_{2M} - L_d)\, e_{1c}}\right]$, respectively, and

$$k_c > L_d,\ \rho_c = \rho_{c0}\frac{1}{2}\ln\frac{k_c + L_d}{k_c - L_d} \tag{55}$$

where, $k_{2M} > L_d$ is the up-bound of k_2 from the system gain limitation; $\rho_{c0} > 1$.

Step 3: Determine the controller parameters k_1, k_2 and ρ through the calculations in Equations (34)∼(38). [Note: When the known reference jumps or suddenly changes, the parameters k_1, k_2 and ρ are updated.]

Step 4: Controller output:

$$u(t) = \begin{cases} k_c\tanh\left[\rho_c(e_2(t) + e_{2c}\ \mathrm{sign}(e_1(t)))\right] - h(t), \text{if } |e_1(t)| > e_{1c}; \\ k_2\tanh[\rho(e_2(t) + k_1e_1(t))] - h(t), \text{if } |e_1(t)| \le e_{1c} \end{cases} \tag{56}$$

https://doi.org/10.1017/aer.2024.50 Published online by Cambridge University Press

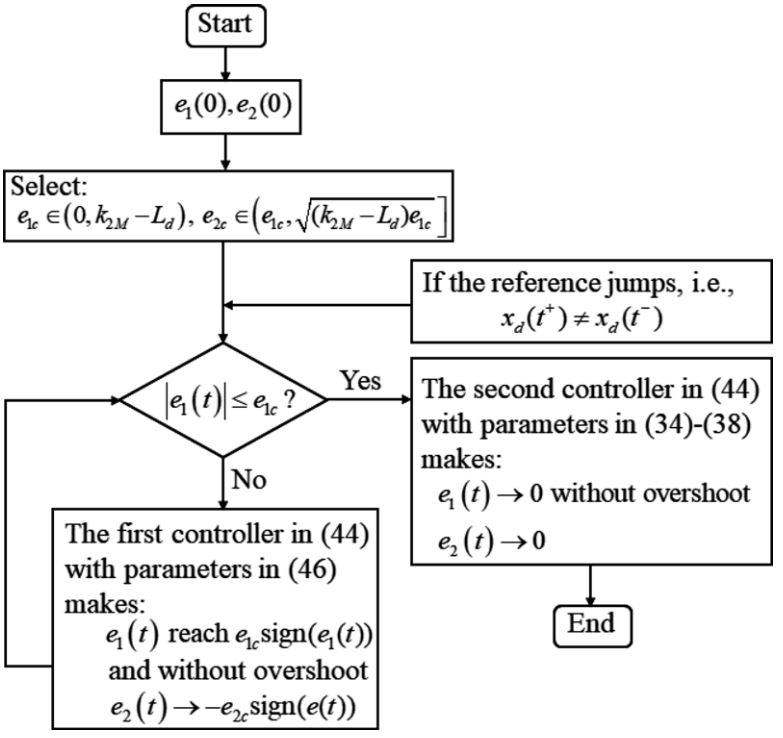

Figure 4. *Flow chart of non-overshooting controller design.*

6.0 Simulation examples on non-overshooting control of uncertain systems

We use two examples to illustrate the non-overshooting control presented in Theorems 5.1 and 5.2, respectively. Consider the uncertain system:

$$\dot{x}_1(t) = x_2(t)$$
$$\dot{x}_2(t) = h(t) + u(t) - \delta(t)$$

where, $h(t) = 5x_1^{\frac{1}{3}}\sin(0.5t)$, and the unknown disturbance or uncertainty $\delta(t) = 1 + 0.3\sin(0.3t)\sin(1.6t)$.

The initial conditions of states: $x_1(0) = 10$, $x_2(0) = -1$

The reference: $x_d(t) = 2 + 0.5\sin(0.8t)$. Therefore, we know that $\dot{x}_d(t) = 0.4\cos(0.8t)$ and $\ddot{x}_d(t) = -0.32\sin(0.8t)$; $x_d(0) = 2$, and $\dot{x}_d(0) = 0.4$.

The upper bound of disturbance/uncertainty: $\sup_{t\in[0,\infty)} |\delta(t)| + \sup_{t\in[0,\infty)} |\ddot{x}_d(t)| = 1.3 + 0.32 = 1.62$, and we can select $L_d = 1.62$.

Define system errors $e_1(t) = x_d(t) - x_1(t)$ and $e_2(t) = \dot{x}_d(t) - x_2(t)$. Then, the error system is:

$$\dot{e}_1(t) = e_2(t)$$
$$\dot{e}_2(t) = -h(t) - u(t) + \ddot{x}_d(t) + \delta(t)$$

and the initial errors are $e_1(0) = x_d(0) - x_1(0) = -8$, and $e_2(0) = \dot{x}_d(0) - x_2(0) = 1.4$.

Suppose the system gain $k_2 \leq k_{2M} = 10$.

Example 6.1: (Non-overshooting control from Theorem 5.1):

(1) *Selection of the desired stable error system*

https://doi.org/10.1017/aer.2024.50 Published online by Cambridge University Press

The sliding mode (18) is selected as the desired stable error system, and

$$\dot{e}_1(t) = e_2(t)$$
$$\dot{e}_2(t) = \begin{cases} -k_c \text{sign}\left[e_2(t) + e_{2c}\text{sign}(e_1(t))\right] + \ddot{x}_d(t) + \delta(t)\,, \text{if} |e_1(t)| > e_{1c}; \\ -k_2 \text{sign}[e_2(t) + k_1 e_1(t)] + \ddot{x}_d(t) + \delta(t)\,, \text{if} |e_1(t)| \le e_{1c} \end{cases}$$

(2) *Determination of parameters k_1 and k_2*

From $e_{1c} \in (0, k_{2M} - L_d) = (0, 8.38)$, we select $e_{1c} = 1$. Then, we get $e_{2c} \in \left(e_{1c}, \sqrt{(k_{2M} - L_d)\, e_{1c}}\right] = \left(1, \sqrt{(10 - 1.62) \times 1}\right] = (1, 2.9]$. We select $e_{2c} = 2$. Select $k_c = 2.5 > L_d$.

According to the parameter determination steps (34)∼(38), we get

$$k_1 = \begin{cases} 0.5\frac{|e_2(t_c)|}{|e_1(t_c)|}, \text{if } e_1(t_c)\, e_2(t_c) < 0 \text{ and } |e_1(t_c)| < |e_2(t_c)|\,; \\ 2.3\frac{|e_2(t_c)|}{|e_1(t_c)|}, \text{if } e_1(t_c)\, e_2(t_c) < 0 \text{ and } |e_1(t_c)| \ge |e_2(t_c)|\,; \\ 2 \in (0, \infty)\,, \text{if others} \end{cases}$$

Adjustment of k_1: $k_1 = 1$ if the calculated $k_1 \in (0, 1)$; and

$$k_2 = \begin{cases} 1.5 \max\left\{k_1 |e_2(t_c)| + L_d, \frac{e_2^2(t_c)}{2|e_1(t_c)|} + L_d\right\}, \text{if } e_1(t_c)\, e_2(t_c) < 0 \text{ and } |e_1(t_c)| < |e_2(t_c)|\,; \\ 1.5 \max\left\{k_1 |e_2(t_c)| + L_d, \frac{k_1^2}{3}\left(|e_1(t_c)| + \sqrt{e_1^2(t_c) + 3\left(\frac{e_2(t_c)}{k_1}\right)^2}\right) + L_d\right\}, \text{if others} \end{cases}$$

where, $e_1(t_c)$ and $e_2(t_c)$ are the initial values of $e_1(t)$ and $e_2(t)$, respectively, when $|e_1(t)| \le e_{1c}$. From the algorithm calculation for the above equations, we can read $k_1 = 1$ and $k_2 = 5.44$.

(3) *Controller design*

According to the controller (40), we get

$$u(t) = \begin{cases} k_c\, \text{sign}\left[e_2(t) + e_{2c}\, \text{sign}(e_1(t))\right] - h(t), \text{if } |e_1(t)| > e_{1c} \\ k_2\, \text{sign}[e_2(t) + k_1 e_1(t)] - h(t), \text{if } |e_1(t)| \le e_{1c} \end{cases}$$

where, $e_{1c} = 1$, $e_{2c} = 2$, $k_c = 2.5$, $k_1 = 1$, $k_2 = 5.44$, and $h(t) = 5x_1^{\frac{1}{3}} \sin(0.5t)$.

(4) *Analysis of simulation results*

The control performance based on the ideal sliding mode is presented in Fig. 5. Figure 5(a) describes the system variable x_1 tracking the reference $x_d(t)$. x_1 tracking $x_d(t)$ is smoothed and non-overshooting, even the unknown time-varying disturbance exists, and the reference is also time variant. Figure 5(b) presents the variable x_2 convergence to the reference derivative $\dot{x}_d(t)$. At the beginning, x_2 increases to speed up the finite-time convergence, then it makes x_1 in the linear convergence law $\dot{e}_1(t) = -k_1 e_1(t)$, and $\lim_{t\to\infty} x_1(t) = x_d(t)$ and $\lim_{t\to\infty} x_2(t) = \dot{x}_d(t)$. Figure 5(c) shows the controller $u(t)$ output. Even the controller can make the system stable and non-overshooting, chattering happens in the controller output, and it may increase actuator trembling.

Example 6.2: (Smoothed non-overshooting control from Theorem 5.2):

(1) *Selection of the desired stable error system*

The smoothed sliding mode (24) is selected as the desired stable error system, and

$$\dot{e}_1(t) = e_2(t)$$
$$\dot{e}_2(t) = \begin{cases} -k_c \tanh\left[\rho_c(e_2(t) + e_{2c}\, \text{sign}(e_1(t)))\right] + \ddot{x}_d(t) + \delta(t), \text{if } |e_1(t)| > e_{1c}; \\ -k_2 \tanh[\rho(e_2(t) + k_1 e_1(t))] + \ddot{x}_d(t) + \delta(t), \text{if } |e_1(t)| \le e_{1c} \end{cases}$$

https://doi.org/10.1017/aer.2024.50 Published online by Cambridge University Press

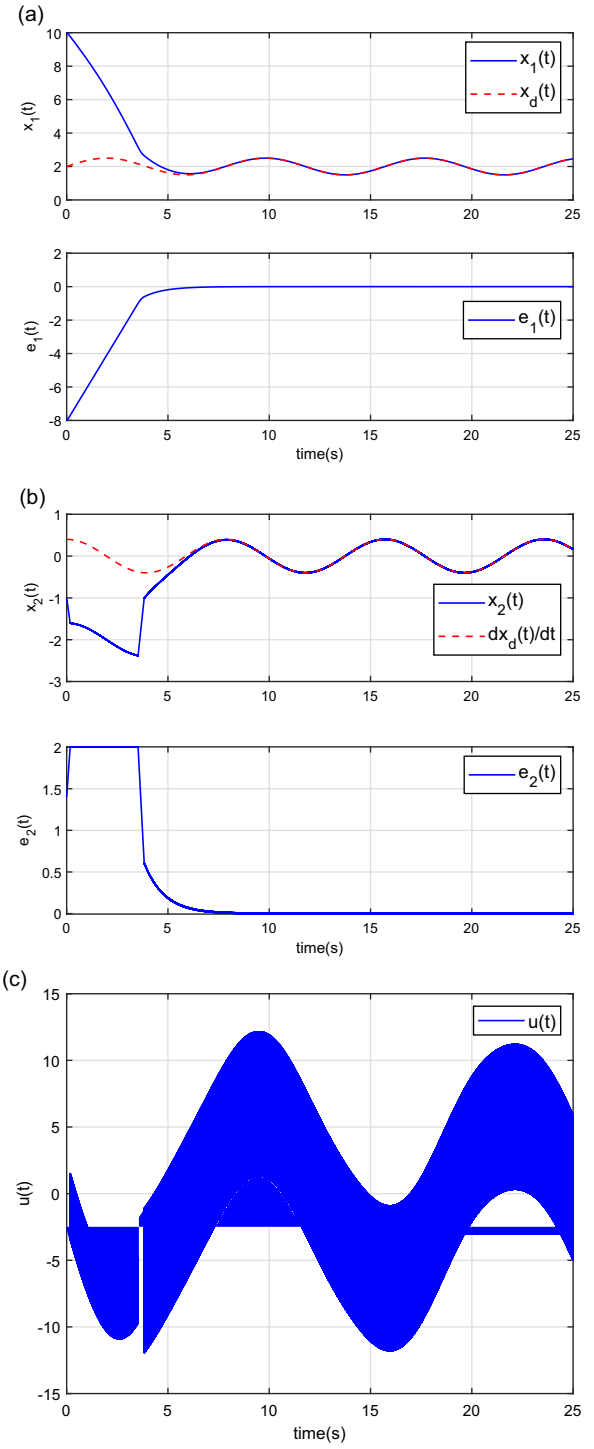

Figure 5. *Example 6.1 Non-overshooting sliding mode control. (a) x_1. (b) x_2. (c) Controller $u(t)$.*

https://doi.org/10.1017/aer.2024.50 Published online by Cambridge University Press

(2) *Determination of parameters k_1, k_2 and ρ according to the parameter determination steps (34)∼(38):*

Select $e_{1c}=1$, $e_{2c}=2$, and $k_c=2.5$. Then, we get $\rho_c=20\frac{1}{2}\ln\frac{k_c+L_d}{k_c-L_d}=15.44$.

Firstly, for determination of k_1 and k_2, we use the same algorithm steps to Example 6.1, and we can read $k_1=1.01$ and $k_2=5.49$.

Secondly, for ρ, we have

$$e_{2\max}=\max\left\{|e_2(t_c)|\,,\frac{k_1}{3}\left[|e_1(t_c)|+\sqrt{e_1^2(t_c)+3\left(\frac{e_2(t_c)}{k_1}\right)^2}\right]\right\}$$

$$\rho=20\max\left\{\frac{1}{2k_1},1\right\}\ln\frac{k_2+k_1e_{2\max}+L_d}{k_2-k_1e_{2\max}-L_d}$$

From the algorithm calculation for the above equations, we can read $\rho=32.19$.

(3) *Controller design*

According to the smoothed controller (44), we get

$$u(t)=\begin{cases}k_c\tanh\left[\rho_c(e_2(t)+e_{2c}\ \mathrm{sign}(e_1(t)))\right]-h(t), \text{ if } |e_1(t)|>e_{1c};\\ k_2\tanh[\rho(e_2(t)+k_1e_1(t))]-h(t), \text{ if } |e_1(t)|\le e_{1c}\end{cases}$$

where, $e_{1c}=1$, $e_{2c}=2$, $k_c=2.5$, $\rho_c=15.44$, $k_1=1.01$, $k_2=5.33$, $\rho=32.19$, and $h(t)=5x_1^{\frac{1}{3}}\sin(0.5t)$.

(4) *Analysis of simulation results*

Figure 6 presents the control performance based on the smoothed sliding mode. Figure 6(a) describes x_1 tracking the reference $x_d(t)$, and Figure 6(b) presents x_2 convergence to the reference derivative $\dot{x}_d(t)$. Even time-varying disturbance exists, and time-variant reference is required, x_1 tracking $x_d(t)$ is smoothed and non-overshooting. Comparing to x_2 in Example 6.1, x_2 in Example 6.2 is smoother. Figure 6(c) shows the smoothed controller $u(t)$ output. The smoothed controller output is beneficial for actuator implementation, and it reduce the actuator trembling.

7.0 UAV Control application

A quadrotor UAV prototype is used [30], which is shown in Fig. 7, and the forces and torques of UAV are described. The system parameters are introduced in Table I.

7.1 Model of UAV flight dynamics [30]

The inertial and fuselage frames are denoted by $\Xi_g=\left(E_x,E_y,E_z\right)$ and $\Xi_b=\left(E_x^b,E_y^b,E_z^b\right)$, respectively; ψ, θ and ϕ are the yaw, pitch and roll angles, respectively. $F_i=b\omega_i^2$ is the thrust force by rotor i, and its reactive torque is $Q_i=k\omega_i^2$. The sum of the four rotor thrusts is $F=\sum_{i=1}^{4}F_i$. The motion equations of the UAV flight dynamics can be expressed by

$$\begin{aligned}\dot{x}_{*1}&=x_{*2}\\ \dot{x}_{*2}&=h_*(t)+\bar{u}_*(t)+\delta_*(t)\end{aligned}\tag{57}$$

where, $*=x,y,z,\psi,\theta,\phi$; $x_{x1}=x$, $x_{y1}=y$, $x_{z1}=z$, $x_{\psi1}=\psi$, $x_{\theta1}=\theta$, $x_{\phi1}=\phi$; $h_x(t)=0$, $h_y(t)=0$, $h_z(t)=-g$, $h_\psi(t)=0$, $h_\theta(t)=0$, $h_\phi(t)=0$; $\delta_x(t)=^{-1}(-k_x\dot{x}+\Delta_x)$; $t)=m^{-1}\left(-k_y\dot{y}+\Delta_y\right)$

https://doi.org/10.1017/aer.2024.50 Published online by Cambridge University Press

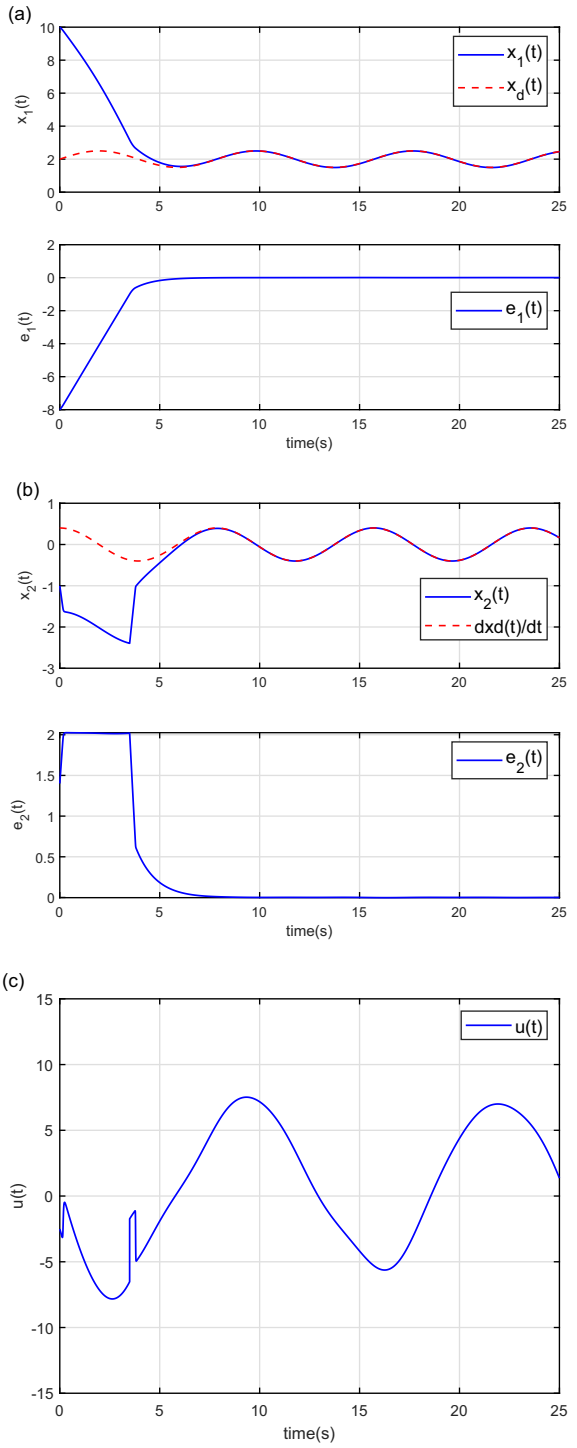

Figure 6. *Example 6.2 Smoothed non-overshooting sliding mode control. (a) x_1. (b) x_2. (c) Controller $u(t)$.*

https://doi.org/10.1017/aer.2024.50 Published online by Cambridge University Press

Table 1. *UAV Parameters [30]*

Symbol	Quantity	Value
m	mass of UAV	2.01 kg
g	gravity acceleration	9.81 m/s^2
l	rotor distance to gravity centre	0.2 m
J_ϕ	moment of inertia about roll	0.25 kg · m^2
J_θ	moment of inertia about pitch	0.25 kg · m^2
J_ψ	moment of inertia about yaw	0.5 kg · m^2
b	rotor force coefficient	2.923×10^{-3}
k	rotor torque coefficient	5×10^{-4}

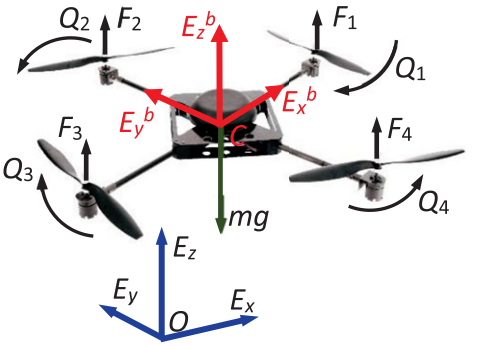

Figure 7. *Forces and torques in UAV [30].*

$\delta_y(t) = m^{-1}\left(-k_y\dot{y} + \Delta_y\right)$; $\delta_z(t) = m^{-1}(-k_z\dot{z} + \Delta_z)$; $\delta_\psi(t) = J_\psi^{-1}\left(-k_\psi\dot{\psi} + \Delta_\psi\right)$; $\delta_\theta(t) = J_\theta^{-1}\left(-lk_\theta\dot{\theta} + \Delta_\theta\right)$; $\delta_\phi(t) = J_\phi^{-1}\left(-lk_\phi\dot{\phi} + \Delta_\phi\right)$; k_x, k_y, k_z, k_ψ, k_θ and k_ϕ are the unknown drag coefficients; $\left(\Delta_x, \Delta_y, \Delta_z\right)$ and $\left(\Delta_\psi, \Delta_\theta, \Delta_\phi\right)$ are the uncertainties in position and attitude dynamics, respectively; $J = diag\left\{J_\psi, J_\theta, J_\phi\right\}$ is the matrix of three-axial moment of inertias; c_θ and s_θ are expressed for cosθ and sinθ, respectively; and

$$\begin{aligned}
\bar{u}_x(t) &= u_x(t)/m = (c_\psi s_\theta c_\phi + s_\psi s_\phi)F/m \\
\bar{u}_y(t) &= u_y(t)/m = (s_\psi s_\theta c_\phi - c_\psi s_\phi)F/m \\
\bar{u}_z(t) &= u_z(t)/m = c_\theta c_\phi F/m \\
\bar{u}_\psi(t) &= u_z(t)/J_\psi = \frac{k}{b}\left(\sum_{i=1}^{4}(-1)^{i+1}F_i\right)/J_\psi \\
\bar{u}_\theta(t) &= u_\theta(t)/J_\theta = (F_3 - F_1)l/J_\theta \\
\bar{u}_\phi(t) &= u_\phi(t)/J_\phi = (F_2 - F_4)l/J_\phi
\end{aligned} \tag{58}$$

7.2 Measurements

A Vicon system provides position and velocity, and a Doppler radar sensor measures height and vertical velocity. An IMU gives the attitude angle and angular velocity. The sensor outputs are:

$$y_{*1}(t) = x_{*1}; y_{*2}(t) = x_{*2} \tag{59}$$

where, $* = x, y, z, \psi, \theta, \phi$.

https://doi.org/10.1017/aer.2024.50 Published online by Cambridge University Press

7.3 Controller design

In this section, the control laws are derived for UAV trajectory tracking and attitude stabilisation.

(1) *Error systems*

The control laws are designed to stabilise the UAV flight. For the desired trajectory ($x_d(t)$, $y_d(t)$, $z_d(t)$) and attitude angle ($\psi_d(t)$, $\theta_d(t)$, $\phi_d(t)$), the error systems of position and attitude dynamics can be expressed, respectively, by

$$\begin{aligned} \dot{e}_{*1}(t) &= \dot{e}_{*2}(t) \\ \dot{e}_{*2}(t) &= -h_*(t) - \bar{u}_*(t) + \ddot{*}_d(t) - \delta_*(t) \end{aligned} \tag{60}$$

where, $e_{*1}(t) = *_d(t) - x_{*1}$, $e_{*2}(t) = \dot{*}_d(t) - x_{*2}$; $* = x, y, z, \psi, \theta, \phi$.

(2) *Controller design*

From (24), we select the smoothed non-overshooting sliding mode as the desired stable, i.e.,

$$\begin{aligned} \dot{e}_{*1}(t) &= e_{*2}(t) \\ \dot{e}_{*2}(t) &= \begin{cases} -k_{*c}\tanh\left[\rho_{*c}(e_{*2}(t) + e_{*2c}\text{sign}(e_{*1}(t)))\right] + \ddot{*}_d(t) - \delta_*(t), \text{if} |e_{*1}(t)| > e_{*1c}; \\ -k_{*2}\tanh[\rho_*(e_{*2}(t) + k_{*1}e_{*1}(t))] + \ddot{*}_d(t) - \delta_*(t), \text{if} |e_{*1}(t)| \le e_{*1c} \end{cases} \end{aligned} \tag{61}$$

In order to turn the error system (60) into the desired stable sliding mode (61), we select

$$\begin{aligned} &-h_*(t) - \bar{u}_*(t) + \ddot{*}_d(t) - \delta_*(t) \\ &= \begin{cases} -k_{*c}\tanh\left[\rho_{*c}(e_{*2}(t) + e_{*2c}\text{sign}(e_{*1}(t)))\right] + \ddot{*}_d(t) - \delta_*(t), \text{if} |e_{*1}(t)| > e_{*1c}; \\ -k_{*2}\tanh[\rho_*(e_{*2}(t) + k_{*1}e_{*1}(t))] + \ddot{*}_d(t) - \delta_*(t), \text{if} |e_{*1}(t)| \le e_{*1c} \end{cases} \end{aligned} \tag{62}$$

Therefore, we get the controller as follows:

$$\bar{u}_*(t) = \begin{cases} k_{*c}\tanh\left[\rho_{*c}(e_{*2}(t) + e_{*2c}\text{sign}(e_{*1}(t)))\right] - h_*(t), \text{if} |e_{*1}(t)| > e_{*1c}; \\ k_{*2}\tanh[\rho_*(e_{*2}(t) + k_{*1}e_{*1}(t))] - h_*(t), \text{if} |e_{*1}(t)| \le e_{*1c} \end{cases} \tag{63}$$

where, $* = x, y, z, \psi, \theta, \phi$. Thus, for the UAV system (57), when the controller (63) is selected, the system is stable, and the system variables x_{*1} (where, $* = x, y, z, \psi, \theta, \phi$) are non-overshooting.

8.0 Experiment on uav non-overshooting control

In this section, an experiment on a quadrotor UAV is presented to demonstrate the proposed non-overshooting control in practice. The UAV prototype shown in Figure 7 is used for the flight test. The flight control system implementation on the hardware is shown in Figure 8, whose elements include: A Gumstix and Arduino Mega 2560 (16MHz) are selected as the driven boards; Gumstix is to collect data from measurements; Arduino Mega is to run control algorithm, which has multiple PWM output channels; a XsensMTI AHRS (10 kHz) provides the 3-axial attitude angles and the angular velocities. A microwave Doppler radar sensor (24GHz) is to detect the height and its vertical velocity. The Vicon system provides position and velocity.

Flight reference trajectory: The UAV reference trajectory includes: (1) take off vertically and hover at the height of 1 m; (2) then cruise along a horizontal line and keep the height; (3) then climb and cruise in a circle with the radius 5m and the height 2.5 m. The 3D reference trajectory is shown in Fig. 9(a).

In the experiment, considering the disturbance (e.g. the crosswind from a swinging electric fan) and the modelling uncertainty in the UAV flight dynamics, the UAV is controlled to track the reference trajectory. The position and velocity are obtained from the Vicon, the height and its vertical velocity

https://doi.org/10.1017/aer.2024.50 Published online by Cambridge University Press

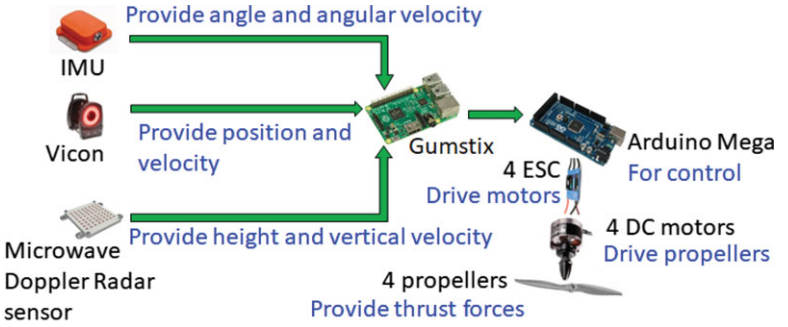

Figure 8. *Control system hardware.*

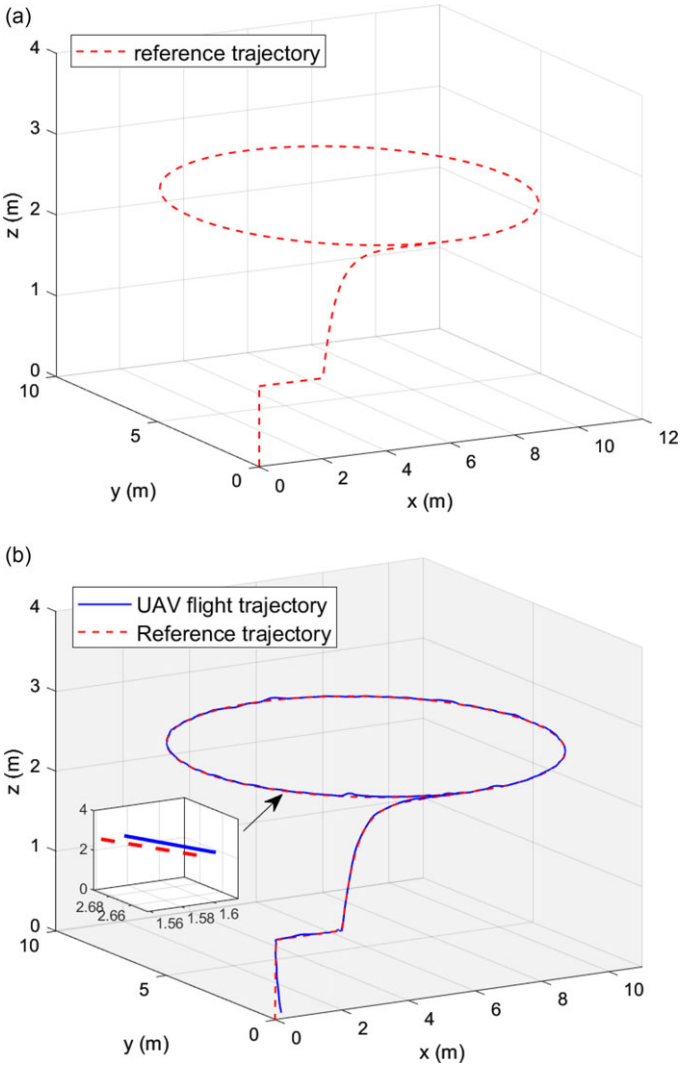

Figure 9. *UAV 3D flight trajectories. (a) Reference trajectory. (b) Flight trajectory comparison.*

https://doi.org/10.1017/aer.2024.50 Published online by Cambridge University Press

are detected by the microwave Doppler radar sensor, and the attitude angle and the angular velocity are measured by the IMU. The controller (63) drives the UAV to track the reference trajectory.

8.1 Controller parameters determination

Through testing the crosswind from the electric fan, and considering the system uncertainties, we estimate the upper bound of disturbances and uncertainties to be within $L_\delta = 4.5\,N$. The up-bound of k_2 is $k_{2M} = 8N$ through the motor tests.

Steps on determination of controller parameters according to (34)∼(38):

Step 1: Measure the initial states, and determine the initial errors.

the initial states:

$x(0) = 0.3, \dot{x}(0) = -0.02;$
$y(0) = 0.2, \dot{y}(0) = -0.01;$
$z(0) = 0.05, \dot{z}(0) = 0.01;$

the initial reference:

$x_d(0) = 0, \dot{x}_d(0) = 0;$
$y_d(0) = 0, \dot{y}_d(0) = 0;$
$z_d(0) = 1, \dot{z}_d(0) = 0;$

then, the initial errors:

$e_{x1}(0) = -0.3, e_{x2}(0) = 0.02;$
$e_{y1}(0) = -0.2, e_{y2}(0) = 0.01;$
$e_{z1}(0) = 0.95, e_{z2}(0) = -0.01.$

Step 2: Select e_{*1c} and e_{*2c} and determine k_{*c} and ρ_{*c}.

From $e_{*1c} \in (0, k_{*2M} - L_\delta) = (0, 3.5)$, we select $e_{*1c} = 1$. Then, we get $e_{*2c} \in \left(e_{*1c}, \sqrt{(k_{*2M} - L_\delta)\, e_{*1c}}\right] = \left(1, \sqrt{(8 - 4.5) \times 1}\right] = (1, 1.87]$. We select $e_{*2c} = 1.2$. Select $k_{*c} = 5.5 > L_\delta$. Then, $\rho_{*c} = 6\frac{1}{2}\ln\frac{k_{*c}+L_{*d}}{k_{*c}-L_{*d}} = 6\frac{1}{2}\ln\frac{5.5+4.5}{5.5-4.5} = 8.83$, where, $* = x, y, z, \psi, \theta, \phi$.

Step 3: Determine the controller parameters k_{*1}, k_{*2} and ρ_* (where, $* = x, y, z, \psi, \theta, \phi$) through the following calculations:

$$k_{*1} = \begin{cases} 0.5\frac{|e_{*2}(t_c)|}{|e_{*1}(t_c)|}, \text{if } e_{*1}(t_c)\, e_{*2}(t_c) < 0 \text{ and } |e_{*1}(t_c)| < |e_{*2}(t_c)|\,; \\ 2.3\frac{|e_{*2}(t_c)|}{|e_{*1}(t_c)|}, \text{if } e_{*1}(t_c)\, e_{*2}(t_c) < 0 \text{ and } |e_{*1}(t_c)| \geq |e_{*2}(t_c)|\,; \\ 2 \in (0, \infty)\,, \text{if others} \end{cases}$$

where, $e_{*1}(t_c)$ and $e_{*2}(t_c)$ are the initial values of $e_{*1}(t)$ and $e_{*2}(t)$, respectively, when $|e_{*1}(t)| \leq e_{*1c}$.

Adjustment of k_{*1}: $k_{*1} = 1$ if the calculated $k_{*1} \in (0, 1)$;

$$k_{*2} = \begin{cases} 1.5 \max\left\{k_{*1}\,|e_{*2}(t_c)| + L_d, \frac{e_{*2}^2(t_c)}{2|e_{*1}(t_c)|} + L_{*d}\right\}, \text{if } e_{*1}(t_c)\, e_{*2}(t_c) < 0 \text{ and } |e_{*1}(t_c)| < |e_{*2}(t_c)|\,; \\ 1.5 \max\left\{k_{*1}\,|e_2(t_c)| + L_{*d}, \frac{k_{*1}^2}{3}\left(|e_{*1}(t_c)| + \sqrt{e_{*1}^2(t_c) + 3\left(\frac{e_{*2}(t_c)}{k_{*1}}\right)^2}\right) + L_{*d}\right\}, \text{if others} \end{cases}$$

$$e_{*2\max} = \max\left\{|e_{*2}(t_c)|\,, \frac{k_{*1}}{3}\left[|e_{*1}(t_c)| + \sqrt{e_{*1}^2(t_c) + 3\left(\frac{e_{*2}(t_c)}{k_{*1}}\right)^2}\right]\right\}$$

$$\rho_* = 3 \max\left\{\frac{1}{2k_{*1}}, 1\right\} \ln\frac{k_{*2} + k_{*1}e_{*2\max} + L_{*d}}{k_{*2} - k_{*1}e_{*2\max} - L_{*d}}$$

https://doi.org/10.1017/aer.2024.50 Published online by Cambridge University Press

Step 4: Controller output (63):

$$\bar{u}_*(t) = \begin{cases} k_{*c}\tanh\left[\rho_{*c}(e_{*2}(t) + e_{*2c}\text{sign}(e_{*1}(t)))\right] - h_*(t), \text{if}|e_{*1}(t)| > e_{1*c}; \\ k_{*2}\tanh[\rho_*(e_{*2}(t) + k_{*1}e_{*1}(t))] - h_*(t), \text{if}|e_{*1}(t)| \le e_{*1c} \end{cases}$$

Because the reference trajectory jumps once at the 6th second, the algorithm in Remark 5.5 updates the controller parameters at this time. From the program algorithm calculation, we can read the two groups of controller parameters as follows:

(1) Parameters for takeoff and hovering for $0 \le t < 6$ (sec):

$$k_{x1} = 1, k_{x2} = 7.05, \rho_x = 4.83$$

$$k_{y1} = 1, k_{y2} = 6.95, \rho_y = 4.83$$

$$k_{z1} = 1, k_{z2} = 7.70, \rho_z = 4.83$$

(2) Parameters for climbing and cruise in a circle for $t \ge 6$ (sec):

$$k_{x1} = 1, k_{x2} = 8.75, \rho_x = 4.83$$

$$k_{y1} = 2, k_{y2} = 6.81, \rho_y = 4.83$$

$$k_{z1} = 2, k_{z2} = 6.94, \rho_z = 4.83$$

8.2. Analysis of UAV control performance

Figure 9(b) gives the UAV 3D flight trajectory comparison. Figures 10, 11 and 12 show the UAV flight trajectories, the tracking errors and the controller outputs in the three directions, respectively: Figure 10 describes the control performance in x-direction; Figure 11 shows the control performance in y-direction; and Figure 12 presents the height control performance in z-direction. From the error outputs, the position errors were within 0.04m, and the velocity errors were within 0.2 m/s.

The position (x, y, z) of the UAV was controlled to track the reference $(x_d(t), y_d(t), z_d(t))$. From the position trajectory outputs in Figures 10, 11 and 12, the smooth and accurate trajectory tracking was achieved with almost no chattering and no overshoot. Even in the presence of time-varying disturbance (i.e. the crosswind from a swinging electric fan), the position and velocity tracking errors remained very small, and there was no overshoot. In addition, by reading the program, we found that although the reference trajectory jumped at the 6th second, the control system re-made the range judgement and the initial value partitioning, and the control parameters were updated at this moment. The UAV remained in the safe flight status throughout the flight.

In this indoor flight test, the bounded time-varying crosswind was generated by a swinging electric fan. Because the up-bound of disturbance was within a certain range, the influence of disturbance was rejected sufficiently by the proposed controller. The experimental environment and test equipment are shown in Ref. [30]. Since the proposed control method only requires that the magnitude of disturbance is within a given range, and it is unrelated to other aspects of the disturbance. For the outdoor flight tests, as long as the magnitude of outdoor wind is within the required range, this control method will be equally effective in suppressing the disturbance.

8.3. Limitations of the proposed method

Through the theoretical analysis (see Theorem 3.1 and Remark 5.3) and the experimental results, we found that the high-frequency noise in the measurements and the bounded stochastic disturbances in the

https://doi.org/10.1017/aer.2024.50 Published online by Cambridge University Press

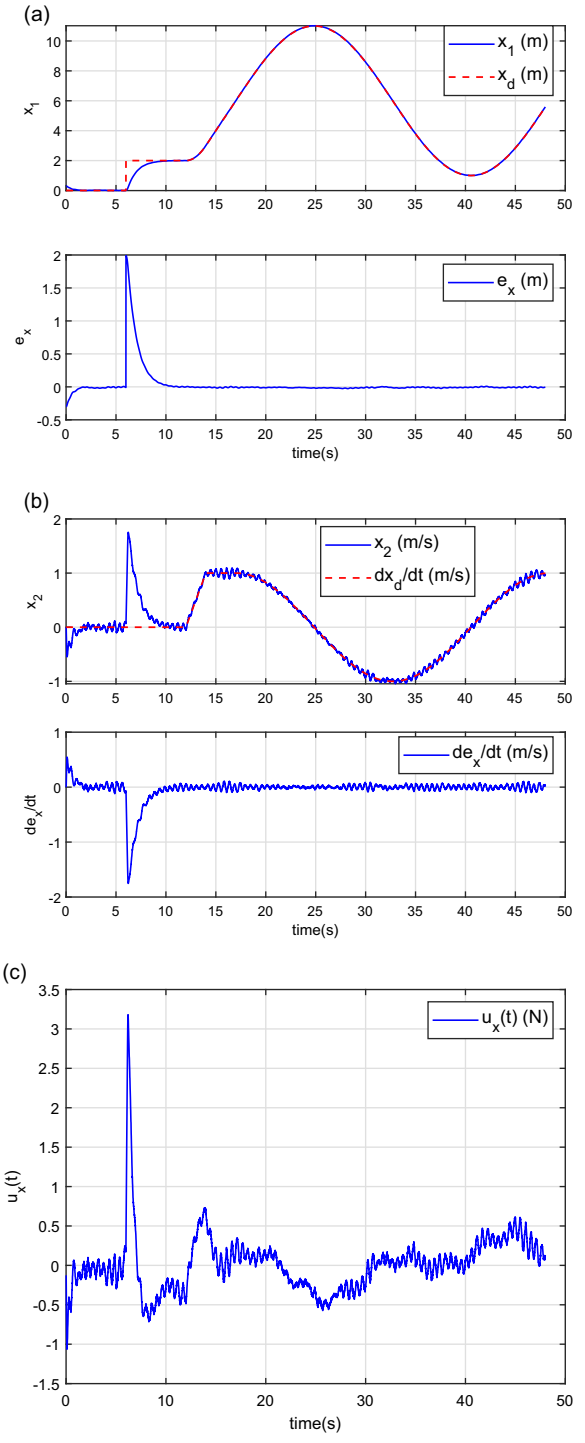

Figure 10. *Control performance in x-direction. (a) x_1. (b) x_2. (c) Controller $u_x(t)$.*

https://doi.org/10.1017/aer.2024.50 Published online by Cambridge University Press

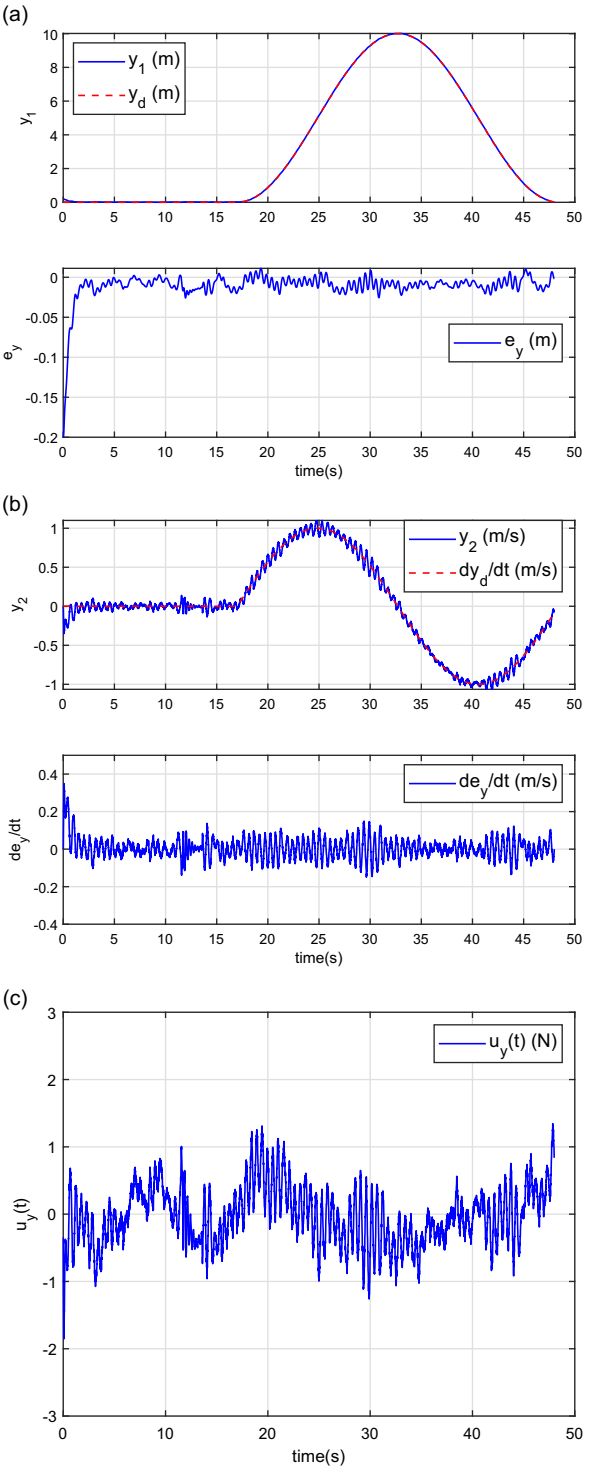

Figure 11. *Control performance in y-direction. (a) y_1. (b) y_2. (c) Controller $u_y(t)$.*

https://doi.org/10.1017/aer.2024.50 Published online by Cambridge University Press

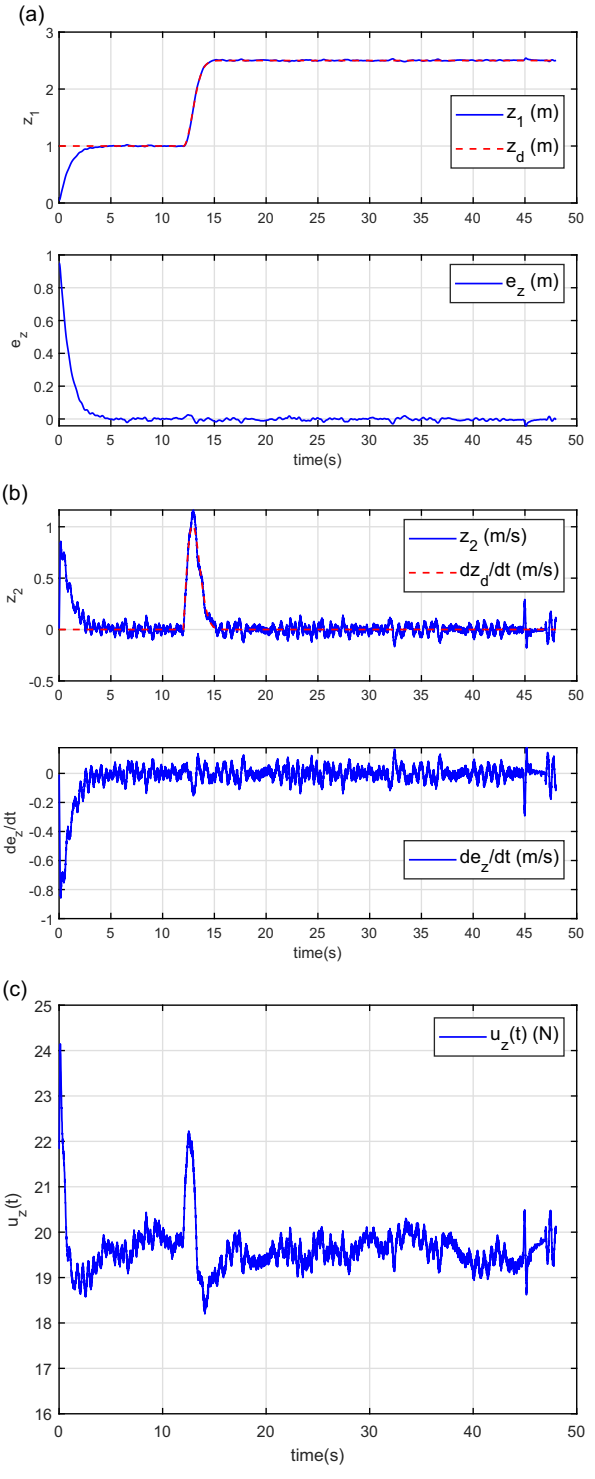

Figure 12. *Control performance in z-direction. (a) z_1. (b) z_2. (c) Controller $u_z(t)$.*

https://doi.org/10.1017/aer.2024.50 Published online by Cambridge University Press

system dynamics almost do not affect the control performance. However, the low-frequency disturbances or errors in the measurements cannot be suppressed effectively by the sliding mode system, resulting in the reduced control accuracy. The potentially effective methods, such as utilising the signal fusion with multiple sensors, can be used to obtain the relatively accurate measurements.

9.0 Conclusions

In this paper, a non-overshooting sliding mode control has been presented to stabilise a class of uncertain systems, and the global non-overshooting stability has been implemented. Even when the bounded stochastic disturbance exists, and the time-variant reference is required, the strict non-overshooting stabilisation is still achieved. The performance of the proposed control method was demonstrated by two simulation examples, and it was applied successfully to a UAV flying test: (1) the high-precision and non-overshooting trajectory tracking was performed; (2) the bounded stochastic disturbances were rejected sufficiently; (3) the bounded and smoothed controller outputs were easily performed by the actuators; (4) the UAV trajectory tracking experiments verified the high maneuverability control capability and non-overshooting performance for the proposed control. The merits of the control method include its global non-overshooting stability, strong robustness and no restriction on the system initial values. Our future work is to optimise the parameters in the proposed controller.

References

[1] Pavel, M.D. Understanding the control characteristics of electric vertical take-off and landing (eVTOL) aircraft for urban air mobility, Aerosp. Sci. Technol., 2022, 125, pp 107–143.
[2] Alan, A., Taylor, A.J., He, C.R., Ames, A.D. and Orosz, G. Control barrier functions and input-to-state safety with application to automated vehicles, *IEEE Trans. Control Syst. Technol.*, 2023, **31**, (6), pp 2744–2759.
[3] Deif, A.M., & ElMaraghy, W.H. A control approach to explore the dynamics of capacity scalability in reconfigurable manufacturing systems, *J. Manuf. Syst.*, 2006, **25**, (1), pp 12–24.
[4] Åström, K.J. and Hägglund, T. Advanced PID Control. ISA-The Instrumentation, Systems and Automation Society, 2006.
[5] Borase, R.P., Maghade, D.K., Sondkar, S.Y. and Pawar, S.N. A review of PID control, tuning methods and applications, *Int. J. Dyn. Control*, 2021, **9**, pp 818–827.
[6] El-Khoury, M., Crisalle, O.D. and Longchamp, R. Influence of zero locations on the number of step-response extrema, *Automatica*, 1993, **29**, (6), pp 1571–1574.
[7] Taghavian, H., Drummond, R. and Johansson, M. Pole-placement for non-overshooting reference tracking, In 2021 60th IEEE Conference on Decision and Control (CDC), 2021, December 13–15, 2021. Austin, Texas, pp 414–421.
[8] Moore K.L., & Bhattacharya S.P. A technique for choosing zero locations for minimal overshoot, *IEEE Trans. Autom. Control*, 1990, **35**, (5), pp 577–580.
[9] Darbha, S. and Bhattacharyya, S.P. On the synthesis of controllers for a non-overshooting step response, *IEEE Trans. Autom. Control*, 2003, **48**, (5), pp 797–800.
[10] Darbha S. On the synthesis of controllers for continuous time LTI systems that achieve a non-negative impulse response, *Automatica.* 2003, **39**, (1), pp 159–165.
[11] Kim Y.C., Keel L.H. and Bhattacharyya S.P. Transient response control via characteristic ratio assignment, *IEEE Trans. Autom. Control*, 2003, **48**, (12), pp 2238–2244.
[12] Bement, M., & Jayasuriya, S. Construction of a set of nonovershooting tracking controllers, *J. Dyn. Sys., Meas., Control*, 2004, **126**, (3), pp 558–567.
[13] Bement, M. and Jayasuriya, S. Use of state feedback to achieve a nonovershooting step response for a class of nonminimum phase systems, *J. Dyn. Sys., Meas., Control*, 2004, **126**, (3), pp 657–660.
[14] Kada, B., Juhany, K.A.T. and Balamesh, A.S.A. Hybrid high-order sliding mode-based control for multivariable cross-coupling systems: Scale-laboratory helicopter system application, *Aeronaut. J.*, 2017, **121**, (1243), pp 1319–1341.
[15] Saied, M., Lussier, B., Fantoni, I., Shraim, H. and Francis, C. Active versus passive fault-tolerant control of a redundant multirotor UAV, *Aeronaut. J.*, 2020, **124**, (1273), pp 385–408.
[16] Wang, X. Sliding mode corrector for jet UAV control, *Aeronaut. J.*, 2024, **128**, (1319), pp 37–72.
[17] González, J.A., Barreiro, B., Dormido, S., & Baños, A. Nonlinear adaptive sliding mode control with fast non-overshooting responses and chattering avoidance, *J. Frank. Inst.*, 2017, **354**, pp 2788–2815.
[18] Tran, T., Ha, Q.P. and Nguyen, H.T. Robust non-overshoot time responses using cascade sliding mode-PID control, *J. Adv. Comput. Intell. Intell. Inform.*, 2007, **11**, (10), pp 1224–1231.
[19] Xavier, N., Bandyopadhyay, B. and Schmid, R. Robust non-overshooting tracking using continuous control for linear multivariable systems, *IET Control Theory Appl.*, 2018, **12**, (7), pp 1006–1011.

https://doi.org/10.1017/aer.2024.50 Published online by Cambridge University Press

[20] Babu, P.S., Xavier, N. and Bandyopadhyay, B. Robust output regulation for state feedback descriptor systems with nonovershooting behavior, *Eur. J. Control*, 2020, **52**, pp 19–25.
[21] Lu, Y.S., Cheng, C.M. and Cheng, C.H. Non-overshooting PI control of variable-speed motor drives with sliding perturbation observers, *Mechatronics*, 2005, **15**, (9), pp 1143–1158.
[22] Cocetti, M., Donnarumma, S., De Pascali, L., Ragni, M., Biral, F., Panizzolo, F., Rinaldi, P.P., Sassaro, A. and Zaccarian, L. Hybrid nonovershooting set-point pressure regulation for a wet clutch, *IEEE/ASME Trans. Mechatron.*, 2020, **25**, (3), pp 1276–1287.
[23] Krstic, M. and Bement, M. Nonovershooting control of strict-feedback nonlinear systems, *IEEE Trans. Autom. Control*, 2006, **51**, (12), pp 1938–1943.
[24] Li, W. and Krstic, M. Mean-nonovershooting control of stochastic nonlinear systems, *IEEE Trans. Autom. Control*, 2021, **66**, (12), pp 5756–5771.
[25] Polyakov, A. and Krstic, M. Homogeneous nonovershooting stabilizers and safety filters rejecting matched disturbances, In 2022 IEEE 61st Conference on Decision and Control (CDC) December 6–9, 2022. Cancún, Mexico, pp 4369–4374.
[26] Polyakov, A. and Krstic, M. Finite-and fixed-time nonovershooting stabilizers and safety filters by homogeneous feedback, *IEEE Trans. Autom. Control*, 2023, **68** (11), pp 6434–6449.
[27] Ding, Y., Guo, Z., Han, Y., Wang, J., Guo, J., Liu, Z. and Zhao, J. Attitude control design for hypersonic reentry vehicles subject to control direction reversal via sliding mode approach, *Int. J. Aeronaut. Space Sci.*, 2023, **25**, (2), pp 563–574.
[28] Sagliano, M., Mooij, E. and Theil S. Adaptive disturbance-based high-order sliding-mode control for hypersonic-entry vehicles, *J. Guid. Control Dyn.*, 2017, **40**, (3), pp 521–536.
[29] Liu Y, Jiang B, Lu J, Cao J and Lu, G. Event-triggered sliding mode control for attitude stabilization of a rigid spacecraft, *IEEE Trans. Syst. Man. Cybern.*, 2018, **50**, (9), pp 3290–3299.
[30] Wang, X. Signal corrector and decoupling estimations for UAV control, *Aeronaut. J.*, 2023, **127**, (1311), pp 796–817.

Appendix

Proof of Lemma 2.1:

Define a new variable

$$z(t) = \int_0^t e(\tau)d\tau - \frac{d}{k_i} \tag{64}$$

Then, we get

$$\dot{z}(t) = e(t), \ddot{z}(t) = \dot{e}(t), \dddot{z}(t) = \ddot{e}(t) \tag{65}$$

Substituting the relations (64) and (65) into system (6), we can rewrite the system (6) as

$$\dddot{z}(t) + k_d\ddot{z}(t) + k_p\dot{z}(t) + k_i z(t) = 0 \tag{66}$$

The characteristic equation of system (66) can be expressed by

$$s^3 + k_d s^2 + k_p s + k_i = 0 \tag{67}$$

According to the stability conditions, for system (67), if k_p, k_i and k_d are selected to make the real parts of all the roots of the characteristic equation (67) negative, then system is exponentially stable, and we get

$$\lim_{t\to\infty} z(t) = 0, \lim_{t\to\infty} \dot{z}(t) = 0, \text{and } \lim_{t\to\infty} \ddot{z}(t) = 0 \tag{68}$$

For (68), from the relations (64) and (65), we get

$$\lim_{t\to\infty} \int_0^t e(\tau)d\tau = \frac{d}{k_i}, \lim_{t\to\infty} e(t) = 0, \text{and } \lim_{t\to\infty} \dot{e}(t) = 0 \tag{69}$$

This concludes the proof. ■

Proof of Lemma 2.2:

Define a new variable

$$z(t) = \int_0^t e(\tau)\tau - \frac{d}{k_i} \tag{70}$$

Then, we get

$$\dot{z}(t) = e(t), \ddot{z}(t) = \dot{e}(t) \tag{71}$$

https://doi.org/10.1017/aer.2024.50 Published online by Cambridge University Press

Substituting the relations (70) and (71) into system (11), we can rewrite the system (11) as

$$\ddot{z}(t) + k_p\dot{z}(t) + k_i z(t) = 0 \tag{72}$$

The characteristic equation of system (72) can be expressed by

$$s^2 + k_p s + k_i = 0 \tag{73}$$

According to the stability conditions, for system (72), if k_p and k_i are selected to make the real parts of all the roots of the characteristic equation (73) negative, then system is exponentially stable, and we get

$$\lim_{t\to\infty} z(t) = 0, \text{ and } \lim_{t\to\infty} \dot{z}(t) = 0 \tag{74}$$

For (74), from the relations (70) and (71), we get

$$\lim_{t\to\infty} \int_0^t e(\tau)d\tau = \frac{d}{k_i}, \text{ and } \lim_{t\to\infty} e(t) = 0 \tag{75}$$

This concludes the proof. ■

Proof of Theorem 3.1:

Proof introduction. The proof on the robust and global non-overshooting stability of the proposed 2-sliding mode is divided into three steps:

A. Robust non-overshooting reachability of the first subsystem. It proves that the first subsystem can make the sliding variables reach a given bounded range and without overshoot. That is to say, the initial values of the second subsystem are compressed to a given bounded range by the first subsystem with robust non-overshooting reachability.

B. Robust non-overshooting stability of the second subsystem. It proves that: conditions on finite-time stability; analytical expressions of sliding variables through partitioning the initial values; and the determination of the bounded parameters for the robust non-overshooting stability.

C. Existence and determination of the initial value range for the second subsystem to obtain the bounded system gains and the non-overshooting stability.

A. Robust non-overshooting reachability of the first subsystem

Case one: If $e_1(t) > e_{1c}$, for system (18), we get

$$\frac{d\,(e_2(t) + e_{2c})}{dt} = -k_c \text{sign}\,[e_2(t) + e_{2c}] + d(t) \tag{76}$$

A Lyapunov function candidate is selected as

$$V_c = \frac{1}{2}(e_2(t) + e_{2c})^2 \tag{77}$$

Then, taking the derivative for V_c, we get

$$\begin{aligned} \dot{V}_c &= (e_2(t) + e_{2c})\,\{-k_c \text{sign}\,[e_2(t) + e_{2c}] + d(t)\} \\ &\le -\,(k_c - L_d)\,|e_2(t) + e_{2c}| = -\sqrt{2}\,(k_c - L_d)\,V_c^{\frac{1}{2}} \end{aligned} \tag{78}$$

We know that $k_c > L_d$. Therefore, there exists a finite time $t_{c1} > 0$, for $t \ge t_{c1}$, such that $e_2(t) = -e_{2c}$. According to $\dot{e}_1 = e_2$, we get that $\dot{e}_1(t) = -e_{2c}$ for $t \ge t_{c1}$. Therefore, there exists a finite time $t_c > 0$, for $t \ge t_c$, such that $e_1(t) \le e_{1c}$.

Case two: If $e_1(t) < -e_{1c}$, for system (18), we get

$$\frac{d\,(e_2(t) - e_{2c})}{dt} = -k_c \text{sign}\,[e_2(t) - e_{2c}] + d(t) \tag{79}$$

https://doi.org/10.1017/aer.2024.50 Published online by Cambridge University Press

Similar method to case $e_1(t) > e_{1c}$, when we select the Lyapunov function candidate as $V_c = \frac{1}{2}(e_2(t) - e_{2c})^2$, we can get that $e_1(t) \geq -e_{1c}$.

Combining cases one and two, we can get that $|e_1(t)| \leq e_{1c}$ for $t \geq t_c$.

B. Robust non-overshooting stability of the second subsystem

In the followig, we discuss the case $|e_1(t)| \leq e_{1c}$.

Finite-time stability conditions

For the sliding mode (18) when $|e_1(t)| \leq e_{1c}$, a Lyapunov function candidate is selected as

$$V_1 = \frac{1}{2}\sigma(t)^2 \tag{80}$$

where, the sliding function $\sigma(t) = e_2(t) + k_1 e_1(t)$. Then, we get

$$\begin{aligned}
\dot{V}_1 &= (e_2(t) + k_1 e_1(t)) \{-k_2 \text{sign}[e_2(t) + k_1 e_1(t)] + d(t) + k_1 e_2(t)\} \\
&= -k_2 |e_2(t) + k_1 e_1(t)| + (k_1 e_2(t) + d(t)) (e_2(t) + k_1 e_1(t)) \\
&\leq -k_2 |e_2(t) + k_1 e_1(t)| + (k_1 |e_2(t)| + L_d) |e_2(t) + k_1 e_1(t)| \\
&= -(k_2 - k_1 |e_2(t)| - L_d) |e_2(t) + k_1 e_1(t)| \\
&= -\sqrt{2}(k_2 - k_1 |e_2(t)| - L_d) V^{\frac{1}{2}}
\end{aligned} \tag{81}$$

If $k_2 > k_1 |e_2(t)| + L_d$, then the sliding mode is finite-time stable. That means there exists a finite time $t_s > 0$, for $t \geq t_c + t_s$, the sliding function $\sigma(t) = e_2(t) + k_1 e_1(t) = 0$. Then, we get the linear convergence law $\dot{e}_1(t) = -k_1 e_1(t)$, and $\lim_{t\to\infty} e_1(t) = 0$.

Trajectories of $e_1(t)$, $e_2(t)$ and $\sigma(t)$ for $t \in [t_c, t_c + t_s)$

For the sliding mode (18), according to the differential inclusion theory, we get

$$\dot{e}_2(t) \in -[k_2 - L_d, k_2 - L_d] \text{sign}[e_2(t) + k_1 e_1(t)] \tag{82}$$

That is to say, there exists $\bar{k}_2 \in [k_2 - L_d, k_2 - L_d]$, such that

$$\dot{e}_2(t) = -\bar{k}_2 \text{sign}[e_2(t) + k_1 e_1(t)] \tag{83}$$

We will determine k_1 and k_2 to make the sign of sliding function $\sigma(t) = e_2(t) + k_1 e_1(t)$ unchanged for $t \in [t_c, t_c + t_s)$, i.e., $\text{sign}[e_2(t) + k_1 e_1(t)] = \text{sign}[e_2(t_c) + k_1 e_1(t_c)]$ for $t \in [t_c, t_c + t_s)$. Then, we can get the simple solution to (83) for $t \in [t_c, t_c + t_s)$, as follows:

$$e_2(t) = e_2(t_c) - \bar{k}_2 \text{sign}[e_2(t) + k_1 e_1(t)] (t - t_c) \tag{84}$$

From $\dot{e}_1(t) = e_2(t)$ in sliding mode (18) and $e_2(t)$ expression in (84), we get

$$e_1(t) = e_1(t_c) + e_2(t_c)(t - t_c) - \frac{1}{2}\bar{k}_2 \text{sign}[e_2(t) + k_1 e_1(t)] \cdot (t - t_c)^2 \tag{85}$$

and

$$\begin{aligned}
\sigma(t) = e_2(t) + k_1 e_1(t) &= e_2(t_c) + k_1 e_1(t_c) - \left(\bar{k}_2 \text{sign}[e_2(t) + k_1 e_1(t)] - k_1 e_2(t_c)\right)(t - t_c) \\
&\quad - \frac{1}{2} k_1 \bar{k}_2 \text{sign}[e_2(t) + k_1 e_1(t)] \cdot (t - t_c)^2
\end{aligned} \tag{86}$$

Non-overshooting convergence conditions

1) For the 2-sliding mode (18), we will determine k_1 and k_2 to generate the two convergence laws: 1) the finite-time convergence law to get the sliding surface $\sigma(t) = e_2(t) + k_1 e_1(t) = 0$ after a finite time $t_c + t_s$; 2) the linear convergence law $\dot{e}_1(t) = -k_1 e_1(t)$ to make $\lim_{t\to\infty} e_1(t) = 0$.

https://doi.org/10.1017/aer.2024.50 Published online by Cambridge University Press

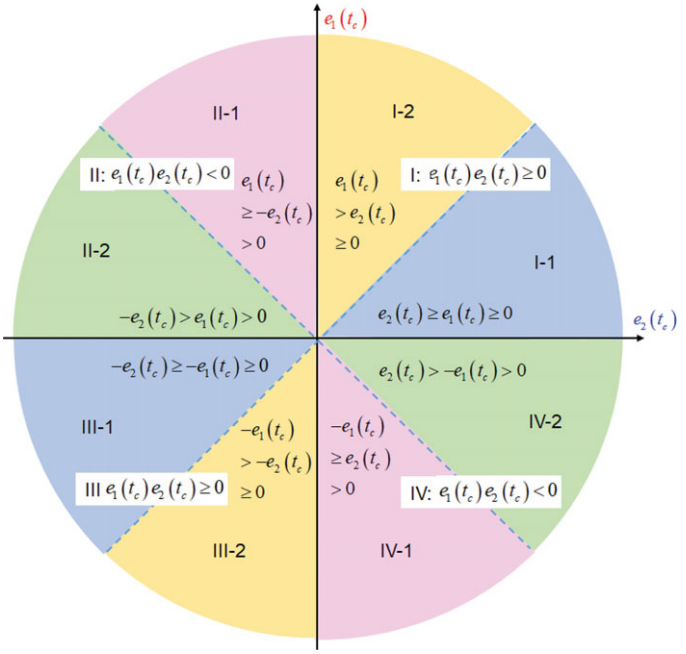

Figure 13. *Partitioning of $e_1(t_c)$ and $e_2(t_c)$ in coordinate.*

2) For the 2-sliding mode (18), in order to get the simple form of sliding variables assumed in (84)–(86), we hope that, for $t \in [t_c, t_c + t_s)$, the sign of sliding function $\sigma(t) = e_2(t) + k_1 e_1(t)$ unchanged as $\sigma(t_c) = e_2(t_c) + k_1 e_1(t_c)$. Thus, function $\text{sign}[e_2(t) + k_1 e_1(t)]$ becomes constant 1 or -1 for $t \in [t_c, t_c + t_s)$. Then, we can get $\dot{e}_2(t) = -\bar{k}_2$ or $\dot{e}_2(t) = \bar{k}_2$ for $t \in [t_c, t_c + t_s)$.

3) For being non-overshooting, $\text{sign}[e_1(t)] = \text{sign}[e_1(t_c)]$ needs always hold until $\lim_{t\to\infty} e_1(t) = 0$.

We know that, the sliding variable $e_1(t)$ is non-overshooting when it is in the convergence law $\dot{e}_1(t) = -k_1 e_1(t)$ for $t \geq t_c + t_s$. Therefore, in order to make $e_1(t)$ non-overshooting during the whole transient process, we only need to guarantee $e_1(t)$ non-overshooting in the finite-time convergence law for $t \in [t_c, t_c + t_s)$.

Partitioning of $e_1(t_c)$ and $e_2(t_c)$ in coordinate

We consider $e_1(t_c)$ and $e_2(t_c)$ in the zones shown in Fig. 13:

1) Zones II-2 and IV-2: $e_1(t_c)\, e_2(t_c) < 0$ with $|e_1(t_c)| < |e_2(t_c)|$
2) Zones IV-1 and II-1: $e_1(t_c)\, e_2(t_c) < 0$ with $|e_1(t_c)| \geq |e_2(t_c)|$
3) Zones III-1 and I-1: $e_1(t_c)\, e_2(t_c) \geq 0$ with $|e_1(t_c)| \leq |e_2(t_c)|$
4) Zones III-2 and I-2: $e_1(t_c)\, e_2(t_c) \geq 0$ with $|e_1(t_c)| > |e_2(t_c)|$

The right side of the sliding mode (18) is the odd function about the origin, therefore, we only consider the convergence performance for the zones (II-2, IV-1, III-1 and III-2). The corresponding zones (IV-2, II-1, I-1 and I-2) about the origin have the same stability performance to the zones (II-2, IV-1, III-1 and III-2), respectively.

Therefore, in the following, we will consider the convergence performance for the following zones:

1) Zone II-2: $-e_2(t_c) > e_1(t_c) > 0$
2) Zone IV-1: $-e_1(t_c) \geq e_2(t_c) > 0$

https://doi.org/10.1017/aer.2024.50 Published online by Cambridge University Press

3) Zone III-1: $-e_2(t_c) \geq -e_1(t_c) \geq 0$
4) Zone III-2: $-e_1(t_c) > -e_2(t_c) \geq 0$

Analytical expressions of sliding variables by assuming the unchanged sign of $\sigma(t) = e_2(t) + k_1 e_1(t)$ *for* $t \in [t_c, t_c + t_s)$

In the selected zones (II-2, IV-1, III-1 and III-2), we will determine k_1 and k_2 to make $\sigma(t) = e_2(t) + k_1 e_1(t) < 0$ for $t \in [t_c, t_c + t_s)$. Then, $\text{sign}[e_2(t) + k_1 e_1(t)] = \text{sign}[e_2(t_c) + k_1 e_1(t_c)] = -1$. Therefore, from (84), (85) and (86), for $t \in [t_c, t_c + t)$, we get the expressions of variables $e_2(t)$, $e_1(t)$ and function $\sigma(t) = e_2(t) + k_1 e_1(t)$, respectively, as follows:

$$e_2(t) = e_2(t_c) + \bar{k}_2 \, (t - t_c) \tag{87}$$

$$e_1(t) = e_1(t_c) + e_2(t_c) \, (t - t_c) + \frac{1}{2}\bar{k}_2 (t - t_c)^2 \overset{\text{define}}{=} c_1 + b_1 \, (t - t_c) + a_1 (t - t_c)^2 \tag{88}$$

$$\begin{aligned} \sigma(t) = e_2(t) + k_1 e_1(t) &= e_2(t_c) + k_1 e_1(t_c) + \left(\bar{k}_2 + k_1 e_2(t_c)\right) (t - t_c) + \frac{1}{2} k_1 \bar{k}_2 (t - t_c)^2 \\ &\overset{\text{define}}{=} c + b \, (t - t_c) + a (t - t_c)^2 \end{aligned} \tag{89}$$

From (88), $e_1(t)$ is a segment of a parabola for $t \in [t_c, t_c + t_s)$, and we get its axis of symmetry:

$$-\frac{b_1}{2a_1} = -\frac{e_2(t_c)}{\bar{k}_2} \tag{90}$$

its vertex:

$$\frac{4a_1 c_1 - b_1^2}{4a_1} = \frac{2\bar{k}_2 e_1(t_c) - e_2^2(t_c)}{2\bar{k}_2} \tag{91}$$

and the time instant when $e_1(t) = 0$:

$$t|_{e_1(t)=0} = \frac{-b_1 + \sqrt{b_1^2 - 4a_1 c_1}}{2a_1} + t_c = -\frac{e_2(t_c)}{\bar{k}_2} + \sqrt{\left(\frac{e_2(t_c)}{\bar{k}_2}\right)^2 - \frac{2e_1(t_c)}{\bar{k}_2}} + t_c \tag{92}$$

From (89), function $\sigma(t) = e_2(t) + k_1 e_1(t)$ is a segment of a parabola for $t \in [t_c, t_c + t_s)$, and we get its axis of symmetry:

$$-\frac{b}{2a} = -\frac{\bar{k}_2 + k_1 e_2(t_c)}{k_1 \bar{k}_2} \tag{93}$$

its vertex:

$$\frac{4ac - b^2}{4a} = \frac{2k_1\bar{k}_2 \left(e_2(t_c) + k_1 e_1(t_c)\right) - \left(\bar{k}_2 + k_1 e_2(t_c)\right)^2}{2k_1 \bar{k}_2} \tag{94}$$

and the time instant when $\sigma(t) = 0$, i.e., the settling time $t_c + t_s$:

$$t_c + t_s = t_c + \frac{-b + \sqrt{b^2 - 4ac}}{2a} = t_c - \left(\frac{1}{k_1} + \frac{e_2(t_c)}{\bar{k}_2}\right) + \sqrt{\frac{1}{k_1^2} + \left(\frac{e_2(t_c)}{\bar{k}_2}\right)^2 - \frac{2e_1(t_c)}{\bar{k}_2}} \tag{95}$$

In the following, for any zone of $e_1(t_c)$ and $e_2(t_c)$, we will determine the parameters k_1 and k_2 to make the sliding mode finite-time stable and $e_1(t)$ non-overshooting for $t \in [t_c, t_c + t_s)$. We know the linear convergence law $\dot{e}_1(t) = -k_1 e_1(t)$ makes the system non-overshooting stable automatically.

Trajectories arrangement of sliding variables: In general, for the different zones of $e_1(t_c)$ and $e_2(t_c)$ shown in Fig. 13, the parameters k_1 and k_2 will be determined to make sliding variables $e_1(t)$, $e_2(t)$ and function $\sigma(t)$ generate the desired convergent trajectories with $e_1(t)$ non-overshooting, shown in Fig. 14:

1) Fig. 14 (a)-1 and (a)-2 are for the zones II-2 and IV-2 in Fig. 13, respectively;

https://doi.org/10.1017/aer.2024.50 Published online by Cambridge University Press

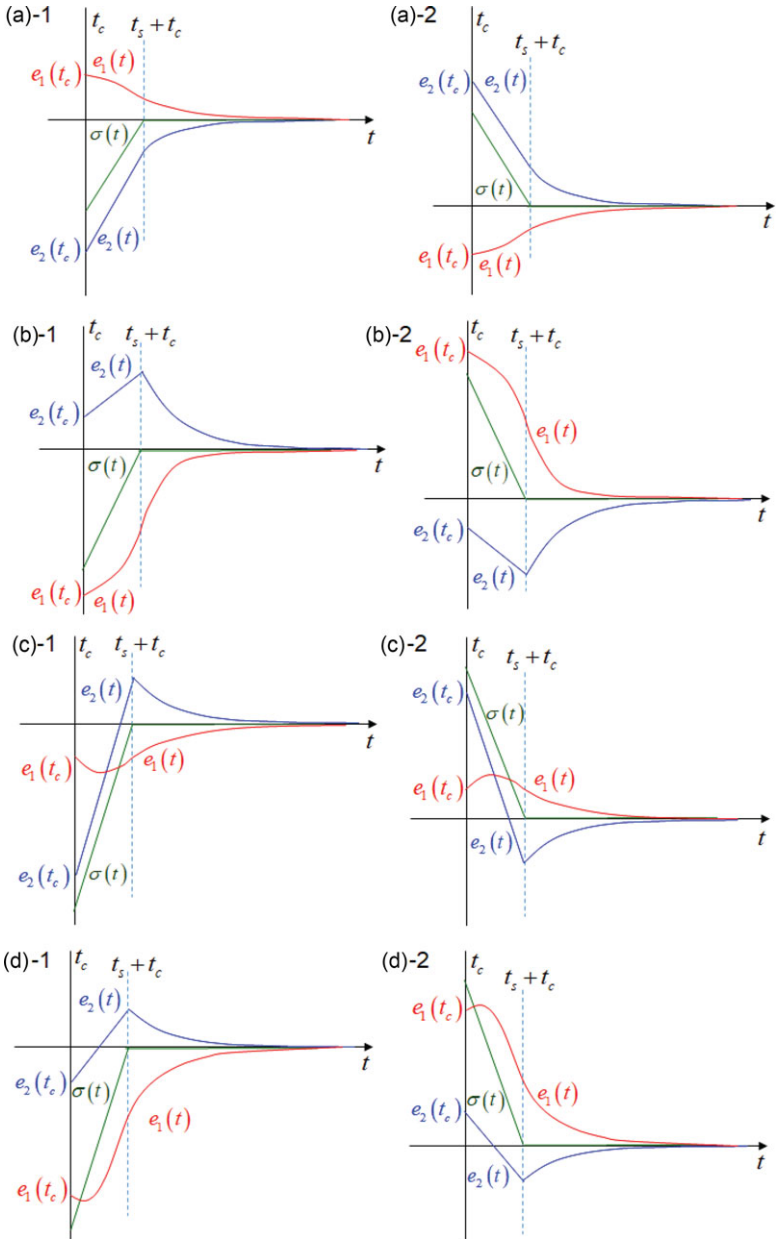

Figure 14. *Arranged trajectories of $e_1(t)$, $e_2(t)$ and $\sigma(t)$ for $e_1(t)$ non-overshooting convergence.*

2) Fig. 14 (b)-1 and (b)-2 are for the zones IV-1 and II-1 in Fig. 13, respectively;
3) Fig. 14 (c)-1 and (c)-2 are for the zones III-1 and I-1 in Fig. 13, respectively; and Fig. 13 (d)-1 and (d)-2 are for zones III-2 and I-2 in Fig. 13, respectively.

Conditions on robust non-overshooting stability
1) For zone II-2: $-e_2(t_c) > e_1(t_c) > 0$
From Figure 13, for zone II-2, we know that the corresponding symmetrical zone is IV-2.
For zone II-2, we can get the conditions of non-overshooting convergence for $t \in [t_c, t_c + t_s)$:

https://doi.org/10.1017/aer.2024.50 Published online by Cambridge University Press

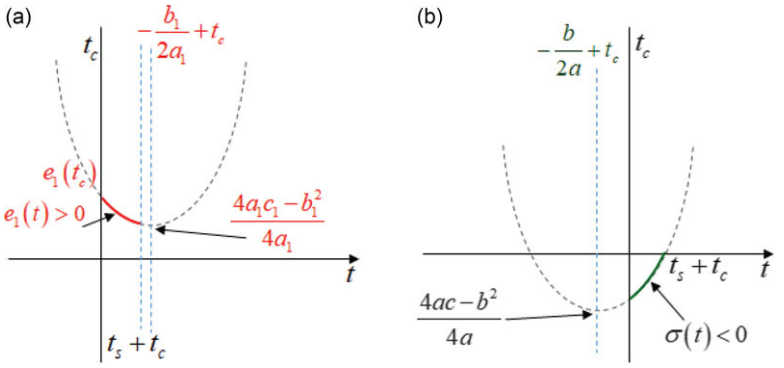

Figure 15. *Arranged trajectories of $e_1(t)$ and $\sigma(t)$ for $e_1(t)$ non-overshooting convergence for $t \in [t_c, t_c + t_s)$ in range II-2: $-e_2(t_c) > e_1(t_c) > 0$.*

1) $\bar{k}_2 > k_1 |e_2(t)|$ [finite-time stability to get convergence law $\dot{e}_1(t) = -k_1 e_1(t)$];
2) the sliding function $\sigma(t) = e_2(t) + k_1 e_1(t) < 0$ for $t \in [t_c, t_c + t_s)$, and $\sigma\ (t_c + t_s) = e_2\ (t_c + t_s) + k_1 e_1\ (t_c + t_s) = 0$;
3) $e_1(t) > 0$ for $t \in [t_c, t_c + t_s)$ [$e_1(t)$ does not go beyond zero];
4) $e_2(t) < 0$ for $t \in [t_c, t_c + t_s)$ [$e_2(t)$ does not go beyond zero].

In the following, we will determine k_1 and k_2 to satisfy these conditions.

From (88), for $e_1(t)$ (a segment of a parabola) for $t \in [t_c, t_c + t_s)$, we get its axis of symmetry

$$-\frac{b_1}{2a_1} = -\frac{e_2(t_c)}{\bar{k}_2} > 0 \tag{96}$$

because $e_2(t_c) < 0$. In order to make $e_1(t) > 0$ for $t \in [t_c, t_c + t_s)$ (See $e_1(t)$ in Figure 15(a)), the vertex needs to satisfy

$$\frac{4a_1c_1 - b_1^2}{4a_1} = \frac{2\bar{k}_2 e_1(t_c) - e_2^2(t_c)}{2\bar{k}_2} > 0 \tag{97}$$

Because $e_1(t_c) > 0$ and $e_2(t_c) < 0$, for (97), the positive $\bar{k}_2$ should satisfy

$$\bar{k}_2 > \frac{e_2^2(t_c)}{2e_1(t_c)} \tag{98}$$

Therefore, from $\bar{k}_2$ in condition (98), we can get that $e_1(t) > 0$ for $t \in [t_c, t_c + t_s)$.

From (89), for the sliding function $\sigma(t) = e_2(t) + k_1 e_1(t)$ (a segment of a parabola) for $t \in [t_c, t_c + t_s)$, we get its axis of symmetry

$$-\frac{b}{2a} = -\frac{\bar{k}_2 + k_1 e_2(t_c)}{k_1 \bar{k}_2} < 0 \tag{99}$$

because of the finite-time convergence condition

$$\bar{k}_2 > -k_1 e_2(t_c) \tag{100}$$

In order to make $\sigma(t) = e_2(t) + k_1 e_1(t) < 0$ for $t \in [t_c, t_c + t_s)$ (See $\sigma(t)$ in Figure 15(b)), the vertex needs to satisfy

$$\frac{4ac - b^2}{4a} = \frac{2k_1\bar{k}_2\ (e_2(t_c) + k_1 e_1(t_c)) - \left(\bar{k}_2 + k_1 e_2(t_c)\right)^2}{2k_1\bar{k}_2} < 0 \tag{101}$$

https://doi.org/10.1017/aer.2024.50 Published online by Cambridge University Press

In order to get the relation in (101), we can let $\sigma(t_c) = e_2(t_c) + k_1 e_1(t_c) < 0$, i.e., $k_1 e_1(t_c) < -e_2(t_c)$. Therefore, we get the condition on k_1, as follows:

$$k_1 < \frac{-e_2(t_c)}{e_1(t_c)} \tag{102}$$

For $e_2(t)$ in (87), we get the time instant when $e_2(t) = 0$ as follows:

$$t|_{e_2(t)=0} = \frac{-e_2(t_c)}{\bar{k}_2} + t_c \tag{103}$$

Comparing the settling time $t_c + t_s$ in (95) and $t|_{e_2(t)=0}$ in (103), we can get

$$t_s + t_c < t|_{e_2(t)=0} \tag{104}$$

Then, it follows that

$$e_2(t) < 0 \text{ for } t \in [t_c, t_c + t_s) \tag{105}$$

We know that zones II-2 and IV-2 have the same convergence performance because of the odd function property in the sliding mode. Therefore, combing (98), (100) and (102), for the zones II-2 (where, $-e_2(t_c) > e_1(t_c) > 0$) and IV-2 (where, $e_2(t_c) > -e_1(t_c) > 0$), we get the non-overshooting convergence conditions, when $e_1(t_c)\, e_2(t_c) < 0$ and $|e_1(t_c)| < |e_2(t_c)|$, as follows:

$$k_1 \in \left(0, \frac{|e_2(t_c)|}{|e_1(t_c)|}\right) \tag{106}$$

$$\bar{k}_2 > \max\left\{k_1 \, |e_2(t_c)| \, , \frac{e_2^2(t_c)}{2\,|e_1(t_c)|}\right\} \tag{107}$$

Furthermore, considering the disturbance $d(t)$, the conditions of parameters selection, when $e_1(t_c)\, e_2(t_c) < 0$ and $|e_1(t_c)| < |e_2(t_c)|$, are expressed as follows:

$$k_1 \in \left(0, \frac{|e_2(t_c)|}{|e_1(t_c)|}\right) \tag{108}$$

$$k_2 > \max\left\{k_1 \, |e_2(t_c)| + L_d, \frac{e_2^2(t_c)}{2e_1(t_c)} + L_d\right\} \tag{109}$$

Therefore, when k_1 and k_2 are selected from (108) and (109), the sliding mode is non-overshooting stable for $t \in [t_c, t_c + t_s)$, and $\sigma(t) = e_2(t) + k_1 e_1(t) = 0$ holds for $t \geq t_c + t_s$. Then, the linear convergence law $\dot{e}_1(t) = -k_1 e_1(t)$ makes $\lim_{t\to\infty} e_1(t) = 0$ without overshoot. In addition, from $\sigma(t) = e_2(t) + k_1 e_1(t) = 0$ for $t \geq t_c + t_s$, we get $\lim_{t\to\infty} e_2(t) = \lim_{t\to\infty} [-k_1 e_1(t)] = 0$.

In general, when $e_1(t_c)$ and $e_2(t_c)$ are in zones II-2 and IV-2, the system is exponentially stable, and no overshoot exists for the variable $e_1(t)$. This confirms the convergence curves of sliding variables $e_1(t)$, $e_2(t)$ and function $\sigma(t)$ described in Figures 14 (a)-1 and (a)-2 for the zones II-2 and IV-2, respectively.

2) For zone IV-1: $-e_1(t_c) \geq e_2(t_c) > 0$

From Figure 13, for zone IV-1, we know that its corresponding symmetrical zone is II-1.

For zone IV-1, we can get the conditions of non-overshooting convergence for $t \in [t_c, t_c + t_s)$:

1) $\bar{k}_2 > k_1 \, |e_2(t)|$ [finite-time stability to get convergence law $\dot{e}_1(t) = -k_1 e_1(t)$]
2) the sliding function $\sigma(t) = e_2(t) + k_1 e_1(t) < 0$ for $t \in [t_c, t_c + t_s)$, and $\sigma\ (t_c + t_s) = e_2\ (t_c + t_s) + k_1 e_1\ (t_c + t_s) = 0$;
3) $e_1(t) < 0$ for $t \in [t_c, t_c + t_s)$ [$e_1(t)$ does not go beyond zero];
4) $e_2(t) > 0$ for $t \in [t_c, t_c + t_s)$ [$e_2(t)$ does not go beyond zero].

In the following, we will determine k_1 and k_2 to satisfy these conditions.

https://doi.org/10.1017/aer.2024.50 Published online by Cambridge University Press

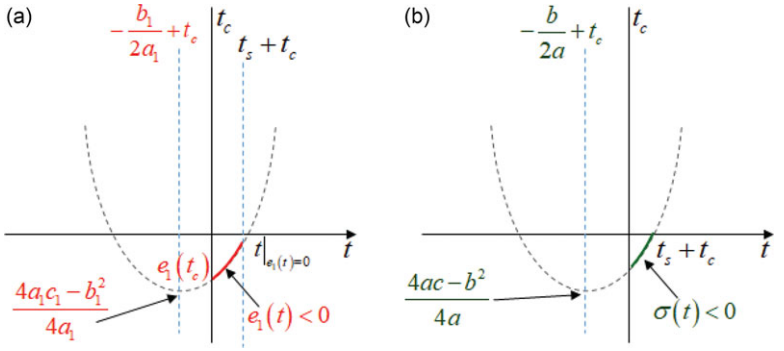

Figure 16. *Arranged trajectories of $e_1(t)$ and $\sigma(t)$ for $e_1(t)$ non-overshooting convergence for $t \in [t_c, t_c + t_s)$ in range IV-1: $-e_1(t_c) \geq e_2(t_c) > 0$.*

From (88), for $e_1(t)$ (a segment of a parabola) for $t \in [t_c, t_c + t_s)$, we get its axis of symmetry

$$-\frac{b_1}{2a_1} = -\frac{e_2(t_c)}{\bar{k}_2} < 0 \tag{110}$$

because $e_2(t_c) > 0$. Also, its vertex satisfies

$$\frac{4a_1c_1 - b_1^2}{4a_1} = \frac{2\bar{k}_2 e_1(t_c) - e_2^2(t_c)}{2\bar{k}_2} < 0 \tag{111}$$

because $e_1(t_c) < 0$ (See $e_1(t)$ in Figure 16(a)).

From (89), for the sliding function $\sigma(t) = e_2(t) + k_1 e_1(t)$ for $t \in [t_c, t_c + t_s)$, its axis of symmetry satisfies

$$-\frac{b}{2a} = -\frac{\bar{k}_2 + k_1 e_2(t_c)}{k_1 \bar{k}_2} < 0 \tag{112}$$

because of the finite-time stability condition:

$$\bar{k}_2 > k_1 \, |e_2(t_c)| \tag{113}$$

In order to make $\sigma(t) = e_2(t) + k_1 e_1(t) < 0$ for $t \in [t_c, t_c + t_s)$ (See $\sigma(t)$ in Figure 16(b)), the vertex needs to satisfy

$$\frac{4ac - b^2}{4a} = \frac{2k_1\bar{k}_2 \left(e_2(t_c) + k_1 e_1(t_c)\right) - \left(\bar{k}_2 + k_1 e_2(t_c)\right)^2}{2k_1\bar{k}_2} < 0 \tag{114}$$

To satisfy (114), we can make $\sigma(t_c) = e_2(t_c) + k_1 e_1(t_c) < 0$ i.e., $-k_1 e_1(t_c) > e_2(t_c)$. Therefore, we get the condition on k_1, as follows:

$$k_1 > \frac{e_2(t_c)}{-e_1(t_c)} \tag{115}$$

Comparing the settling time $t_c + t_s$ in (95) and $t|_{e_1(t)=0}$ in (92), we get

$$t_c + t_s < t|_{e_1(t)=0} \tag{116}$$

Therefore, we get

$$e_1(t) < 0 \text{ for } t \in [t_c, t_c + t_s) \tag{117}$$

For $e_2(t)$, when $t = t_c + t_s$, from (87) and (95), we get

$$e_2(t)|_{t=t_c+t_s} = e_2(t_c) + \bar{k}_2 t_s = -\frac{\bar{k}_2}{k_1} + \sqrt{e_2^2(t_c) + \left(\frac{\bar{k}_2}{k_1}\right)^2 - 2\bar{k}_2 e_1(t_c)} \tag{118}$$

https://doi.org/10.1017/aer.2024.50 Published online by Cambridge University Press

For $t \in [t_c, t_c + t_s)$, considering the finite-time convergence condition, we need

$$\bar{k}_2 > k_1 \max\{|e_2(t)|\} = k_1 \left| e_2(t)|_{t=t_c+t_s} \right| \tag{119}$$

Combining (118) and (119), we get

$$\bar{k}_2 > k_1 \left| e_2(t)|_{t=t_c+t_s} \right| = k_1 \left| -\frac{\bar{k}_2}{k_1} + \sqrt{e_2^2(t_c) + \left(\frac{\bar{k}_2}{k_1}\right)^2 - 2\bar{k}_2 e_1(t_c)} \right| \tag{120}$$

Therefore, $\bar{k}_2$ should satisfy

$$\bar{k}_2 > \frac{k_1^2}{3}\left[|e_1(t_c)| + \sqrt{e_1^2(t_c) + 3\left(\frac{e_2(t_c)}{k_1}\right)^2} \right] \tag{121}$$

We know that zones IV-1 and II-1 have the same convergence performance because of the odd function property in the sliding mode. Therefore, combing (113), (115) and (121), for the zones IV-1 (where, $-e_1(t_c) \geq e_2(t_c) > 0$) and II-1 (where, $e_1(t_c) \geq -e_2(t_c) > 0$), we get the non-overshooting convergence conditions, when $e_1(t_c)\, e_2(t_c) < 0$ and $|e_1(t_c)| \geq |e_2(t_c)|$, as follows:

$$k_1 \in \left(\frac{|e_2(t_c)|}{|e_1(t_c)|}, \infty \right) \tag{122}$$

$$\bar{k}_2 > \max\left\{ k_1 |e_2(t_c)|, \frac{k_1^2}{3}\left[|e_1(t_c)| + \sqrt{e_1^2(t_c) + 3\left(\frac{e_2(t_c)}{k_1}\right)^2} \right] \right\} \tag{123}$$

Furthermore, considering the disturbance $d(t)$, the conditions of parameters selection, when $e_1(t_c)\, e_2(t_c) < 0$ and $|e_1(t_c)| \geq |e_2(t_c)|$, are expressed as follows:

$$k_1 \in \left(\frac{|e_2(t_c)|}{|e_1(t_c)|}, \infty \right) \tag{124}$$

$$k_2 > \max\left\{ k_1 |e_2(t_c)| + L_d, \frac{k_1^2}{3}\left[|e_1(t_c)| + \sqrt{e_1^2(t_c) + 3\left(\frac{e_2(t_c)}{k_1}\right)^2} \right] + L_d \right\}, \tag{125}$$

Therefore, the sliding mode is non-overshooting stable for $t \in [t_c, t_c + t_s)$, and $\sigma(t) = 0$ holds for $t \geq t_c + t_s$. Then, the linear convergence law $\dot{e}_1(t) = -k_1 e_1(t)$ makes $\lim_{t\to\infty} e_1(t) = 0$ without overshoot. In addition, from $e_2(t) + k_1 e_1(t) = 0$ for $t \geq t_c + t_s$, we get $\lim_{t\to\infty} e_2(t) = 0$.

In general, for $e_1(t_c)$ and $e_2(t_c)$ in zones IV-1 and II-1, when k_1 and k_2 are selected from (124) and (125), the system is exponentially stable, and no overshoot exists for the variable $e_1(t)$. This confirms the convergence curves of sliding variables $e_1(t)$, $e_2(t)$ and function $\sigma(t)$ described in Fig. 14 (b)-1 and (b)-2 for the zones IV-1 and II-1, respectively.

3) For zone III, i.e., III-1: $-e_2(t_c) \geq -e_1(t_c) \geq 0$ and III-2: $-e_1(t_c) > -e_2(t_c) \geq 0$

From Figure 13, we know that the corresponding symmetrical zone of III is zone I; and the corresponding symmetrical zone of III-2 is zone I-2.

For zone III, we can get the conditions of non-overshooting convergence for $t \in [t_c, t_c + t_s)$:

1) $\bar{k}_2 > k_1 |e_2(t)|$ [finite-time stability to get convergence law $\dot{e}_1(t) = -k_1 e_1(t)$];
2) the sliding function $\sigma(t) = e_2(t) + k_1 e_1(t) < 0$ for $t \in [t_c, t_c + t_s)$, and $\sigma\ (t_c + t_s) = e_2\ (t_c + t_s) + k_1 e_1\ (t_c + t_s) = 0$;
3) $e_1(t) < 0$ [$e_1(t)$ does not go beyond zero].

In the following, we will determine k_1 and k_2 to satisfy these conditions.

https://doi.org/10.1017/aer.2024.50 Published online by Cambridge University Press

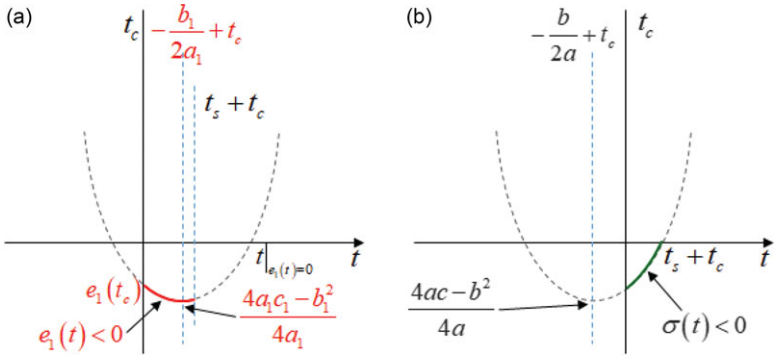

Figure 17. *Arranged trajectories of $e_1(t)$ and $\sigma(t)$ for $e_1(t)$ non-overshooting convergence for $t \in [t_c, t_c + t_s)$ in range III-1: $-e_2(t_c) \geq -e_1(t_c) \geq 0$ and range III-2: $-e_1(t_c) > -e_2(t_c) \geq 0$.*

From (88), for $e_1(t)$ (a segment of a parabola) for $t \in [t_c, t_c + t_s)$, we get its axis of symmetry

$$-\frac{b_1}{2a_1} = -\frac{e_2(t_c)}{\bar{k}_2} \geq 0 \tag{126}$$

because $e_2(t_c) \leq 0$. Also, its vertex satisfies

$$\frac{4a_1c_1 - b_1^2}{4a_1} = \frac{2\bar{k}_2 e_1(t_c) - e_2^2(t_c)}{2\bar{k}_2} < 0 \tag{127}$$

because $e_1(t_c) \leq 0$ (See $e_1(t)$ in Figure 17(a)).

From (89), for $\sigma(t) = e_2(t) + k_1 e_1(t)$ (the segment of a parabola) for $t \in [t_c, t_c + t_s)$, we get its axis of symmetry:

$$-\frac{b}{2a} = -\frac{\bar{k}_2 + k_1 e_2(t_c)}{k_1 \bar{k}_2} < 0 \tag{128}$$

because of the finite-time convergence condition

$$\bar{k}_2 > k_1 \, |e_2(t_c)| \tag{129}$$

In order to make $\sigma(t) = {}_2(t) + k_1 e_1(t) < 0$ for $t \in [t_c, t_c + t_s)$ (See Figure 17(b)), its vertex needs to satisfy

$$\frac{4ac - b^2}{4a} = \frac{2k_1\bar{k}_2 \left(e_2(t_c) + k_1 e_1(t_c)\right) - \left(\bar{k}_2 + k_1 e_2(t_c)\right)^2}{2k_1\bar{k}_2} < 0 \tag{130}$$

To satisfy (130), it should be that $\sigma(t_c) = e_2(t_c) + k_1 e_1(t_c) < 0$. Therefore, for zones III, we get the k_1 condition as

$$k_1 > 0 \tag{131}$$

Comparing the settling time $t_c + t_s$ in (95) and $t|_{e_1(t)=0}$ in (92), we get

$$t_c + t_s < t|_{e_1(t)=0} \tag{132}$$

Therefore, we get

$$e_1(t) < 0 \text{ for } t \in [t_c, t_c + t_s) \tag{133}$$

For $e_2(t)$, when $t = t_c + t_s$, from (87) and (95), we get

$$e_2(t)|_{t=t_c+t_s} = e_2(t_c) - \bar{k}_2 t_s = -\frac{\bar{k}_2}{k_1} + \sqrt{e_2^2(t_c) + \left(\frac{\bar{k}_2}{k_1}\right)^2 - 2\bar{k}_2 e_1(t_c)} \tag{134}$$

https://doi.org/10.1017/aer.2024.50 Published online by Cambridge University Press

For $t \in [t_c, t_c + t_s)$, considering the finite-time convergence condition, we need

$$\bar{k}_2 > k_1 \max\{|e_2(t)|\} = k_1 \left| e_2(t)|_{t=t_c+t_s} \right| \tag{135}$$

Combining (134) and (135), we get

$$\bar{k}_2 > k_1 \left| e_2(t)|_{t=t_c+t_s} \right| = k_1 \left| -\frac{\bar{k}_2}{k_1} + \sqrt{e_2^2(t_c) + \left(\frac{\bar{k}_2}{k_1}\right)^2 - 2\bar{k}_2 e_1(t_c)} \right| \tag{136}$$

Therefore, $\bar{k}_2$ should satisfy

$$\bar{k}_2 > \frac{k_1^2}{3}\left[|e_1(t_c)| + \sqrt{e_1^2(t_c) + 3\left(\frac{e_2(t_c)}{k_1}\right)^2} \right] \tag{137}$$

We know that zones III and I have the same convergence performance because of the odd function property in the sliding mode. Therefore, combing (129), (131) and (137), for the zones III and I, we get the non-overshooting convergence conditions:

$$k_1 \in (0, \infty) \tag{138}$$

$$\bar{k}_2 > \max\left\{ k_1 |e_2(t_c)|\,, \frac{k_1^2}{3}\left[|e_1(t_c)| + \sqrt{e_1^2(t_c) + 3\left(\frac{e_2(t_c)}{k_1}\right)^2} \right] \right\} \tag{139}$$

Furthermore, considering the disturbance $d(t)$, the conditions of parameters selection are expressed as follows:

$$k_1 \in (0, \infty) \tag{140}$$

$$k_2 > \max\left\{ k_1 |e_2(t_c)| + L_d, \frac{k_1^2}{3}\left[|e_1(t_c)| + \sqrt{e_1^2(t_c) + 3\left(\frac{e_2(t_c)}{k_1}\right)^2} \right] + L_d \right\} \tag{141}$$

Therefore, the sliding mode is non-overshooting stable for $t \in [t_c, t_c + t_s)$, and $\sigma(t) = 0$ holds for $t \geq t_c + t_s$. Then, the linear convergence law $\dot{e}_1(t) = -k_1 e_1(t)$ makes $\lim_{t\to\infty} e_1(t) = 0$ without overshoot. In addition, from $e_2(t) + k_1 e_1(t) = 0$ for $t \geq t_c + t_s$, we get $\lim_{t\to\infty} e_2(t) = 0$.

In general, for $e_1(t_c)$ and $e_2(t_c)$ in zones III and I, when k_1 and k_2 are selected from (140) and (141), the system is exponentially stable, and no overshoot exists for the variable $e_1(t)$. This confirms the convergence curves of sliding variables $e_1(t)$, $e_2(t)$ and function $\sigma(t)$ described in Fig. 13 (c)-1 and (c)-2 for the zones III-1 and I-1, and Fig. 13 (d)-1 and (d)-2 for zones III-2 and I-2, respectively.

Finally, combing parameter selection conditions (108)–(109), (124)–(125), and (140)–(141) in the different zones, we can get the parameter conditions (19) and (20) for non-overshooting stable system in Theorem 3.1.

C. Determination of e_{1c} and e_{2c} for bounded system gain and without overshoot

From the expression of k_2 in (20), in order to make the system gain bounded, we need to reduce $|e_1(t_c)|$, $|e_2(t_c)|$ and $\frac{e_2^2(t_c)}{2|e_1(t_c)|}$. For the first subsystem, according to the robust and non-overshooting reachability, we get $e_{1c} = e_1(t_c)$ and $e_{2c} = e_2(t_c)$ when $t = t_c$. Therefore, we can select the bounded e_{1c} and e_{2c} for bounded $|e_1(t_c)|$ and $|e_2(t_c)|$. Furthermore, we hope to get the fast convergence as the mode in the zones II-1 and IV-1, and the up-bound of k_2 from the system gain limitation is considered. In order to get the non-overshooting stability with the bounded system gain, we select

$$\begin{aligned} e_{1c} &\in (0, k_{2M} - L_d) \\ e_{2c} &\in \left(e_{1c}, \sqrt{(k_{2M} - L_d)\, e_{1c}} \right] \end{aligned} \tag{142}$$

https://doi.org/10.1017/aer.2024.50 Published online by Cambridge University Press

where, k_{2M} is the up-bound of k_2. In fact, due to $e_{1c} = e_1(t_c)$ and $e_{2c} = e_2(t_c)$ when $t = t_c$, we get the parameter $k_1 \in \left(0, \frac{e_{2c}}{e_{1c}}\right)$ for the second subsystem. Therefore, there exists $\beta_{11} \in (0, 1)$ such that $k_1 = \beta_{11}\frac{e_{2c}}{e_{1c}}$. In (20), we know that

$$k_1 e_{2c} \le k_{2M} - L_d \tag{143}$$

From $k_1 = \beta_{11}\frac{e_{2c}}{e_{1c}}$ and (143), we can get

$$\beta_{11}\frac{e_{2c}^2}{e_{1c}} \le k_{2M} - L_d \tag{144}$$

In (20), we also know that

$$\frac{e_{2c}^2}{2e_{1c}} \le k_{2M} - L_d \tag{145}$$

Combing (144) and (145), we can select

$$\max\left\{\beta_{11}, \frac{1}{2}\right\}\frac{e_{2c}^2}{e_{1c}} \le k_{2M} - L_d \tag{146}$$

Because the system gain limitation $0 < k_2 \le k_{2M}$, i.e., k_{2M} is the maximum implementation of k_2. Because $\beta_{11} \in (0, 1)$, we get $\max\left\{\beta_{11}, \frac{1}{2}\right\} < 1$. Therefore, from $e_{1c} < e_{2c}$, for (146), we select

$$e_{1c} < e_{2c} \le \sqrt{(k_{2M} - L_d)\, e_{1c}} \tag{147}$$

i.e., $e_{1c}^2 < (k_{2M} - L_d)\, e_{1c}$ and $e_{1c} < e_{2c} \le \sqrt{(k_{2M} - L_d)\, e_{1c}}$. Then, we get (142).
This concludes the proof. ■

Proof of Theorem 3.2:
(i) Firstly, we consider $|e_1(t)| > e_{1c}$.
Case one: If $e_1(t) > e_{1c}$, for (24), we get

$$\frac{d\,(e_2(t) + e_{2c})}{dt} = -k_c \tanh\left[\rho_c\,(e_2(t) + e_{2c})\right] + d(t) \tag{148}$$

A Lyapunov function candidate is selected as

$$V_c = \frac{1}{2}(e_2(t) + e_{2c})^2 \tag{149}$$

Then, taking the derivative for V_c, we get

$$\begin{aligned}\dot{V}_c &= (e_2(t) + e_{2c})\left\{-k_c \tanh\left[\rho_c\,(e_2(t) + e_{2c})\right] + d(t)\right\} \\ &\le -\left(k_c\left|\tanh\left[\rho_c\,(e_2(t) + e_{2c})\right]\right| - L_d\right)|e_2(t) + e_{2c}| \\ &= -\sqrt{2}\left(k_c\left|\tanh\left[\rho_c\,(e_2(t) + e_{2c})\right]\right| - L_d\right)V_c^{\frac{1}{2}}\end{aligned} \tag{150}$$

From (150), if $\left|\tanh\left[\rho_c\,(e_2(t) + e_{2c})\right]\right| > \frac{L_d}{k_c}$, then $\dot{V}_c(t) < 0$, and $|e_2(t) + e_{2c}|$ decreases, and we get

$$\left|\tanh\left[\rho_c\,(e_2(t) + e_{2c})\right]\right| \le \frac{L_d}{k_c} \tag{151}$$

i.e.,

$$\left|1 - \frac{2}{e^{2\rho_c(e_2(t)+e_{2c})} + 1}\right| \le \frac{L_d}{k_c} \tag{152}$$

Therefore, there exists a finite time $t_{c1} > 0$, for $t \ge t_{c1}$, such that

$$|e_2(t) + e_{2c}| \le \frac{1}{2\rho_c}\ln\frac{k_c + L_d}{k_c - L_d} \tag{153}$$

https://doi.org/10.1017/aer.2024.50 Published online by Cambridge University Press

Because $\rho_c \gg \frac{1}{2}\ln\frac{k_c+L_d}{k_c-L_d}$, we get $|e_2(t)+e_{2c}| \ll 1$. There exists $|O(1/\rho)| \le \frac{1}{2\rho_c}\ln\frac{k_c+L_d}{k_c-L_d}$, such that $e_2(t) = -e_{2c} + O(1/\rho)$. From $\dot{e}_1 = e_2$, we get $\dot{e}_1 = -e_{2c} + O(1/\rho_c)$ for $t \ge t_{c1}$. Therefore, there exists a finite time $t_{c2} > t_{c1} > 0$, for $t \ge t_{c2}$, such that $e_1(t) \le e_{1c}$.

We know that $k_c > L_d$. Therefore, there exists a finite time $t_{c1} > 0$, for $t \ge t_{c1}$, such that $e_2(t) = -e_{2c}$. According to $\dot{e}_1 = e_2$, we get that $\dot{e}_1(t) = -e_{2c}$ for $t \ge t_{c1}$. Therefore, there exists a finite time $t_c > 0$, for $t \ge t_c$, such that $e_1(t) \le e_{1c}$.

Case two: If $e_1(t) < -e_{1c}$, for (24), we get

$$\frac{d\,(e_2(t)-e_{2c})}{dt} = -k_c\tanh\left[\rho_c\,(e_2(t)-e_{2c})\right] + d(t) \tag{154}$$

Similar method to case $e_1(t) > e_{1c}$, when we select the Lyapunov function candidate as $V_c = \frac{1}{2}(e_2(t)-e_{2c})^2$, there exists a finite time $t_c > 0$, for $t \ge t_c$, such that $e_1(t) \ge -e_{1c}$.

Combining cases one and two, we can get that $|e_1(t)| \le e_{1c}$ for $t \ge t_c$.

In the following, we discuss the sliding mode system when $|e_1(t)| \le e_{1c}$.

For the smoothed sliding mode (24), a Lyapunov function candidate is selected as

$$V_2(t) = \frac{1}{2}[e_2(t)+k_1e_1(t)]^2 \tag{155}$$

Then, taking the derivative for $V_2(t)$, we get

$$\begin{aligned}
\dot{V}_2 &= [e_2(t)+k_1e_1(t)]\left\{-k_2\tanh\left[\rho\,(e_2(t)+k_1e_1(t))\right] - d(t) + k_1e_2(t)\right\}\\
&\le -k_2\,[e_2(t)+k_1e_1(t)]\,|\tanh\left[\rho\,(e_2(t)+k_1e_1(t))\right]|\,\mathrm{sign}\,[e_2(t)+k_1e_1(t)]\\
&\quad + (k_1\,|e_2(t)| + L_d)\,|e_2(t)+k_1e_1(t)|\\
&= -\left(k_2\,|\tanh\left[\rho\,(e_2(t)+k_1e_1(t))\right]| - k_1\,|e_2(t)| - L_d\right)|e_2(t)+k_1e_1(t)|\\
&= -\left(k_2\,|\tanh\left[\rho\,(e_2(t)+k_1e_1(t))\right]| - k_1\,|e_2(t)| - L_d\right)V^{\frac{1}{2}}(t)
\end{aligned} \tag{156}$$

From (156), if $|\tanh\left[\rho\,(e_2(t)+k_1e_1(t))\right]| > \frac{k_1|e_2(t)|+L_d}{k_2}$, then $\dot{V}_2(t) < 0$, and $|e_2(t)+k_1e_1(t)|$ decreases. We know that, the function $|\tanh\left[\rho\,(e_2(t)+k_1e_1(t))\right]|$ is the the monotonically increasing function about $|e_2(t)+k_1e_1(t)|$. Therefore, $|e_2(t)+k_1e_1(t)|$ decreases until

$$|\tanh\left[\rho\,(e_2(t)+k_1e_1(t))\right]| \le \frac{k_1\,|e_2(t)|+L_d}{k_2} \tag{157}$$

We define

$$\max\{|e_2(t)|\} = \max\left\{|e_2(t_c)|\,,\,\frac{k_1}{3}\left[|e_1(t_c)| + \sqrt{e_1^2(t_c)+3\left(\frac{e_2(t_c)}{k_1}\right)^2}\right]\right\} \overset{\text{define}}{=} e_{2\max} \tag{158}$$

For (157), from (158), we get

$$\left|1 - \frac{2}{e^{2\rho[e_2(t)+k_1e_1(t)]}+1}\right| \le \frac{k_1e_{2\max}+L_d}{k_2} \tag{159}$$

Function $e_2 + k_1e_1 < 0$ holds for $t \in [t_c, t_c+t_s)$ in the zones (II-2, IV-1, III-1 and III-2). Therefore, (159) can be expressed by

$$\frac{2}{e^{2\rho[e_2(t)+k_1e_1(t)]}+1} - 1 \le \frac{k_1e_{2\max}+L_d}{k_2} \tag{160}$$

Then, it follows that

$$|e_2(t)+k_1e_1(t)| \le \frac{1}{2\rho}\ln\frac{k_2+k_1e_{2\max}+L_d}{k_2-k_1e_{2\max}-L_d} \tag{161}$$

From the relation $\dot{e}_1(t) = e_2(t)$ in the sliding mode (24), for (161), there exists a function $\beta(t)$, where $|\beta(t)| \le \frac{1}{2\rho}\ln\frac{k_2+k_1e_{2\max}+L_d}{k_2-k_1e_{2\max}-L_d}$, such that the following convergence law holds:

$$\dot{e}_1(t) = -k_1e_1(t) + \beta(t) \tag{162}$$

https://doi.org/10.1017/aer.2024.50 Published online by Cambridge University Press

The solution to the convergence law (162) is

$$e_1(t) = \left(\int_{t_c}^{t} \beta(\tau) e^{k_1 \tau} d\tau \right) \; e^{-k_1 t} \tag{163}$$

Therefore, we get

$$|e_1(t)| \le |\beta(\tau)| \left(\int_{t_c}^{t} \mathrm{e}^{k_1 \tau} d\tau \right) \mathrm{e}^{-k_1 t} \le \frac{1}{2\rho k_1} \ln \frac{k_2 + k_1 e_{2\max} + L_d}{k_2 - k_1 e_{2\max} - L_d} \left(1 - \mathrm{e}^{-k_1 (t - t_c)} \right) \tag{164}$$

Then, it follows that

$$\lim_{t \to \infty} |e_1(t)| \le \frac{1}{2\rho k_1} \ln \frac{k_2 + k_1 e_{2\max} + L_d}{k_2 - k_1 e_{2\max} - L_d} \tag{165}$$

Because $\rho \gg \frac{1}{2k_1} \ln \frac{k_2 + k_1 e_{2\max} + L_d}{k_2 - k_1 e_{2\max} - L_d}$ is selected, the up-bound of $\lim_{t \to \infty} |e_1(t)|$ is sufficiently small, and $\frac{1}{2\rho k_1} \ln \frac{k_2 + k_1 e_{2\max} + L_d}{k_2 - k_1 e_{2\max} - L_d} \ll 1$ holds. For $e_2(t)$, from (161) and (164), we have

$$\begin{aligned} |e_2(t)| &= |e_2(t) + k_1 e_1(t) - k_1 e_1(t)| \le |e_2(t) + k_1 e_1(t)| + k_1 \, |e_1(t)| \\ &\le \frac{1}{2\rho} \ln \frac{k_2 + k_1 e_{2\max} + L_d}{k_2 - k_1 e_{2\max} - L_d} + \frac{1}{2\rho} \ln \frac{k_2 + k_1 e_{2\max} + L_d}{k_2 - k_1 e_{2\max} - L_d} \left(1 - \mathrm{e}^{-k_1 (t - t_c)} \right) \end{aligned} \tag{166}$$

Therefore, we get

$$\lim_{t \to \infty} |e_2(t)| \le \frac{1}{\rho} \ln \frac{k_2 + k_1 e_{2\max} + L_d}{k_2 - k_1 e_{2\max} - L_d} \tag{167}$$

Because $\rho \gg \ln \frac{k_2 + k_1 e_{2\max} + L_d}{k_2 - k_1 e_{2\max} - L_d}$ is selected, the up-bound of $\lim_{t \to \infty} |e_2(t)|$ is sufficiently small, and $\frac{1}{\rho} \ln \frac{k_2 + k_1 e_{2\max} + L_d}{k_2 - k_1 e_{2\max} - L_d} \ll 1$ holds.

(ii) Specially, when ρ is selected large enough, i.e., $\rho \to +\infty$, the sliding variable up-bounds in (165) and (167) approach to zero, and

$$\lim_{t \to \infty} \lim_{\rho \to +\infty} e_1(t) = 0 \text{and} \lim_{t \to \infty} \lim_{\rho \to +\infty} e_2(t) = 0$$

From $\lim_{\rho \to +\infty} \tanh(\rho \cdot x) = \text{sign}(x)$, the tanh-function-based sliding mode (24) becomes the ideal 2-sliding mode (18). This concludes the proof. ■

Proof of Theorem 5.1:

Define $e_1(t) = x_d(t) - x_1(t)$ and $e_2(t) = \dot{x}_d(t) - x_2(t)$. Then, the error system is

$$\begin{aligned} \dot{e}_1(t) &= e_2(t) \\ \dot{e}_2(t) &= -h(t) - u(t) + \ddot{x}_d(t) + \delta(t) \end{aligned} \tag{168}$$

The desired stable sliding mode (18) in Theorem 3.1 is selected, where, $d(t) = \ddot{x}_d(t) + \delta(t)$. In order to turn the error system (168) into the sliding mode (18), we select

$$\begin{aligned} \dot{e}_2(t) &= -h(t) - u(t) + \ddot{x}_d(t) + d(t) \\ &= \begin{cases} -k_c \text{sign} \left[e_2(t) + e_{2c} \text{sign} \left(e_1(t) \right) \right] + \ddot{x}_d(t) + \delta(t), \text{if } |e_1(t)| > e_{1c}; \\ -k_2 \text{sign} \left[e_2(t) + k_1 e_1(t) \right] + \ddot{x}_d(t) + \delta(t), \text{if } |e_1(t)| \le e_{1c} \end{cases} \end{aligned} \tag{169}$$

Therefore, we get the controller as follows:

$$u(t) = \begin{cases} k_c \text{sign} \left[e_2(t) + e_{2c} \text{sign} \left(e_1(t) \right) \right] - h(t), \text{if } |e_1(t)| > e_{1c} \\ k_2 \text{sign} \left[e_2(t) + k_1 e_1(t) \right] - h(t), \text{if } |e_1(t)| \le e_{1c} \end{cases} \tag{170}$$

Thus, for the uncertain system (39), when the controller (40) is selected, the system is stable, and x_1 tracking $x_d(t)$ is non-overshooting. This concludes the proof. ■

https://doi.org/10.1017/aer.2024.50 Published online by Cambridge University Press

Proof of Theorem 5.2:
Define $e_1(t) = x_d(t) - x_1(t)$ and $e_2(t) = \dot{x}_d(t) - x_2(t)$. Then, the error system is

$$\begin{aligned} \dot{e}_1(t) &= e_2(t) \\ \dot{e}_2(t) &= -h(t) - u(t) + \ddot{x}_d(t) + \delta(t) \end{aligned} \tag{171}$$

The desired stable sliding mode (24) in Theorem 3.2 is selected, where, $d(t) = \ddot{x}_d(t) + \delta(t)$. In order to turn the error system (171) into the sliding mode (24), we select

$$\begin{aligned} \dot{e}_2 &= -h(t) - u(t) + \ddot{x}_d(t) + d(t) \\ &= \begin{cases} -k_c \tanh\left[\rho_c \left(e_2(t) + e_{2c}\text{sign}\left(e_1(t)\right)\right)\right] + \ddot{x}_d(t) + \delta(t), \text{if } |e_1(t)| > e_{1c}; \\ -k_2 \tanh\left[\rho \left(e_2(t) + k_1 e_1(t)\right)\right] + \ddot{x}_d(t) + \delta(t), \text{if } |e_1(t)| \le e_{1c} \end{cases} \end{aligned} \tag{172}$$

Therefore, we get the controller as follows:

$$u(t) = \begin{cases} k_c \tanh\left[\rho_c \left(e_2(t) + e_{2c}\text{sign}\left(e_1(t)\right)\right)\right] - h(t), \text{if } |e_1(t)| > e_{1c}; \\ k_2 \tanh\left[\rho \left(e_2(t) + k_1 e_1(t)\right)\right] - h(t), \text{if } |e_1(t)| \le e_{1c} \end{cases} \tag{173}$$

Thus, for the uncertain system (39), when the controller (44) is selected, the system is stable, and x_1 tracking $x_d(t)$ is non-overshooting. This concludes the proof. ■

Cite this article: Wang X. and Mao X. Non-overshooting sliding mode for UAV control. *The Aeronautical Journal*, https://doi.org/10.1017/aer.2024.50